J Solution Chem (2013) 42:2409–2442
DOI 10.1007/s10953-013-0116-5

Complex Formation Equilibria and Molecular Structure of Divalent Metal Ions–Vitamin B3–Glycine Oligopeptides Systems

Aisha Y. Rajhi · Yi-Hsu Ju · Artik E. Angkawijaya · Ahmed E. Fazary

Received: 13 July 2013 / Accepted: 24 September 2013 / Published online: 21 November 2013

Abstract Complex formation of divalent transition metal ions (copper(II), cobalt(II) and nickel(II)), vitamin B3 (nicotinic acid) and glycine oligopeptides (glycine, glycylglycine, glycyl-L-phenylalanine, and glycylglycylglycine) were studied at 298 K in aqueous solutions using the pH-potentiometric technique. The copper Cu(II), cobalt Co(II), and nickel Ni(II) complexing capacity of vitamin B3 in the absence and in the presence of glycine peptides and their overall stability constants in aqueous solutions were obtained and explained by the HYPERQUAD 2008 program using the potentiometric data. From the protonation and complex formation constants, representative complex species distribution diagrams were obtained using HYSS 2009 software. The UV–Vis spectroscopic, cyclic voltammeteric and conductometric titration measurements were carried out to give qualitative information about the conformation of the complexes formed in these solutions and their stoichiometric ratios. The Gibbs energies and the molecular structures of the complexes were evaluated and predicted using Gaussian 09 software molecular modeling and density functional theory calculations.

Keywords Niacin · Potentiometry · Spectrophotometry · Cyclic voltammetery · Conductometry · Gaussian 09

A. Y. Rajhi · A. E. Fazary
Chemistry Department, Faculty of Science, King Khalid University, Abha 9004, Kingdom of Saudi Arabia

Y.-H. Ju · A. E. Angkawijaya
Department of Chemical Engineering, National Taiwan University of Science and Technology, 43 Keelung Road, Section 4, Taipei 106-07, Taiwan
e-mail: yhju@mail.ntust.edu.tw

A. E. Fazary (✉)
Applied Research Sector, Egyptian Organization for Biological Products and Vaccines (VACSERA Holding Company), 51 Wezaret El-Zeraa St., Agouza, Giza, Egypt
e-mail: aefazary@gmail.com; afazary@kku.edu.sa

1 Introduction

Vitamin B3 ($C_6H_5NO_2$, known as nicotinic acid (NA), niacin, and vitamin PP) is a one of eight water-soluble B complex vitamins and has two other forms, niacinamide (nicotinamide) and inositol hexanicotinate, which have different biological effects from vitamin B3 [1]. It is known that B vitamins help the body to convert food (carbohydrates) into fuel (glucose), which is used to produce energy [2, 3], help the nervous system function properly [4], help the body to use fats and proteins [5], and they are needed for healthy skin, hair, eyes, and liver [6, 7]. Recently, it was found that vitamin B3 also helps the body make various sex and stress-related hormones in the adrenal glands and other parts of the body [8], lower elevated LDL ("bad") cholesterol and triglyceride (fat) levels in the blood [9], and also help improve circulation [10]. We have studied complex formation between divalent and trivalent metal ions and amino, non-protein amino, and phenolic acids, and vitamins in aqueous solutions in the presence of some non-protein amino acids or soluble vitamins [11–16].

A thorough literature review showed that no work seems to have been reported on the study of complexation between metal ions, vitamins and glycine (G) oligopeptides peptides in aqueous solutions. Herein, the stability constants of divalent metal ions–vitamin B3 acids (NA)–G peptides complexes in binary and mixed ligand systems were determined by pH-potentiometric titrations in aqueous solutions. The measurements were done at 298.15 K in solutions with an ionic strength 0.15 mol·dm^{-3} $NaNO_3$ and the data analyses were done using the Hyperquad 2008 computational program. Also, complex species formation in aqueous solutions was confirmed by UV–Vis spectroscopic, cyclic voltammetric and conductometric measurements. Finally, Gibbs energies and the molecular structures of the complexes were calculated using the Gaussian 09 program.

2 Experimental Section

2.1 Chemicals and Solutions

All chemicals were analytical grade and were used without further purification. NA ($C_6H_5NO_2$) was purchased from Aldrich (Germany) with 99.0 % purity. G containing peptides (G, glycylglycine (GG), glycyl-L-phenylalanine (GP) and glycylglycylglycine (GGG)) used were analytical grade chemicals with purity 99.0 % and were produced by Sigma (Germany). Nitric acid (Panreac, Spain) solutions was prepared and standardized before used. Copper chloride dihydrate ($CuCl_2{\cdot}2H_2O$, 99.0 % purity) was a product of Kanto Chemical Co., Inc. (Japan). Nickel chloride hexahydrate ($NiCl_2{\cdot}6H_2O$, 97.0 % purity) and cobalt nitrate hexahydrate ($Co(NO_3)_2{\cdot}6H_2O$, 99.0 % purity) were obtained from Acros Organics, USA. Sodium nitrate ($NaNO_3$, 99.0 % purity) from Acros Organics (USA) was used. Carbonate-free sodium hydroxide solution was prepared by dissolving NaOH pellets (Across Organics, USA) with ultra-pure water and the solution was potentiometrically standardized against potassium hydrogen phthalate with purity 99.0 % (Aldrich, USA). All solutions were freshly prepared daily. Chemicals were accurately weighed then dissolved in ultra-pure water (NANO pure-Ultrapure water that was deionized with 18.3 MΩ·cm^{-1} resistance and distilled).

2.2 pH-Potentiometric Titrations

2.2.1 Titration Procedures

The pH-potentiometric measurements of G peptides (P) in the absence or presence of divalent metal ions and NA ligands were performed using a Metrohm 702 SM titrator, equipped with a 664 Dosimate, 728 magnetic stirrer, coupled with a Dosino burette model 683. The electrode response can be read to the third decimal in terms of pH units with a precision of ±0.001 mV. Prior to each titration, the pH-automatic titrinometer was calibrated with standard buffer solutions at three pH values ~4.00, 7.00 and 9.00. The burette's volume droplet calibration was also carried out daily to increase the experiment accuracy. All the pH-potentiometric titrations were carried out in a 150 cm^3 double walled equilibrium cell in which the temperature and ionic strength of the solutions were maintained at 298.15 K (by a thermostated circulating bath) and 0.15 $mol{\cdot}dm^{-3}$ using $NaNO_3$ solution. Titrations for different binary metal–ligand complex stability constant determination were carried out at various concentration ratios (T_M:T_L = 1:1, 1:2, 1:3, M = Cu(II), Co(II), and Ni(II), L = NA, G, GG, GP, and GGG), while titrations for mixed ligand complexes were carried out at concentration ratios T_M : T_{LP}: T_{LNA} = 1:1:1, (where P (peptide unit) = G, GG, GP, and GGG ligands, L_{NA} = NA ligand). Each titration was repeated at least three times with reproducibility ±0.02 pH units and was done in pH range ~2.5 to 11. The titrator was coupled to a personal computer and the titration software TINET version 2.4 was used to control the titration data acquisition [17].

2.2.2 pH-Potentiometric Data Analysis

The HYPERQUAD2008 program was used to derive protonation and complex stability constants from the potentiometric data [18]. For this purpose, a fitting criterion based on minimization of the non-linear least-squares sum, defined by the difference between the calculated and the experimental data of the titration curves, was used:

$$x^2 = \frac{\sum \left(E_{\text{cal}} - E_{\text{exp}}\right)^2}{E_{\text{cal}}} \tag{1}$$

These constants are presented as $\log_{10}$ values of the overall formation constant ($\log_{10} \beta_{pqrs}$) and expressed by the following equation:

$$p\text{M} + q\text{A} + r\text{P} + s\text{H} \rightleftharpoons \text{M}_p\text{A}_q\text{P}_r\text{H}_s$$

$$\beta_{pqrs} = \frac{\left[\text{M}_p\text{A}_q\text{P}_r\text{H}_s\right]}{[\text{M}]^p[\text{A}]^q[\text{P}]^r[\text{H}]^s} \tag{2}$$

where M = Cu(II), Co(II), and Ni(II), A = NA, P = G, GG, GP, and GGG. HYPER QUAD 2008 permits the determination of formation constants of different complex species in solution simultaneously [18]. Various models, with different complexes, were examined and the model that gave the best statistical fit and and was chemically sensible was chosen. Besides HYPERQUAD 2008, the Hyperquad Simulation and Speciation (HySS 2009) program was also used to provide complex speciation distribution diagrams [19].

2.3 Density Functional Theory Calculations

In this work, the Gaussian 09 program was used to predict the structures of the complexes [20]. The structures were optimized using density functional theory with Becke's three-parameter hybrid [21] with the correlation of Lee–Yang–Parr, LYP (B3LYP) method [22] and the 6-31 + G(d) basis set was used [23, 24]. Along with the geometry optimization, the frequency analysis was done to obtain the thermochemistry properties of the complexes. The B3LYP/6-31 + G(d) basis set was chosen since it shown to be one of the suitable basis set to approach the molecular orbital of metal complexes [22–27]. The validity of the structures optimization was checked by using normal-mode frequency analysis, in which the real minimum structure must exhibit positive values for all frequencies. The modeling was performed by employing a number of assumptions as simplification, such as the usage of fully deprotonated ligands, only considering the complex formation of one metal ion and one ligand, and not considering the usage of salt to maintain the solution's ionic strength.

2.4 UV–Vis Spectrophotometric Measurements

Divalent metal ion complex species were spectrophotometrically studied in solutions at 298 K using a compact, double-beam Shimadzu UV-1800 UV/Vis Scanning Spectrophotometer with standard 1 cm quartz cells. UV/Vis bandwidth, scan speed and data interval used are 0.1 nm, 100 nm·min^{-1} and 1.0 nm, respectively. These solutions were prepared with the same metal-to-ligand molar ratio as done previously for the pH-potentiometric titrations and were analyzed at the pH where the maximum amounts of binary and mixed ligand complexes are formed.

2.5 Conductometric Measurements

The conductometric titrations were carried out using a Techne conductivity meter (model 4510), to investigate the stoichiometries of the complex species. The following mixture was titrated conductometrically against a 0.10 mol·dm^{-3} NaOH solution: 3×10^{-3} mol·dm^{-3} HNO_3 + 0.15 mol·dm^{-3} $NaNO_3$ + 1×10^{-3} mol·dm^{-3} ligand (L = NA, G, GG, GP, or GGG) + 1×10^{-3} mol·dm^{-3} metal ion (M = Cu(II), Co(II), or Ni(II)) for each binary complex species, while conductometric titrations for various mixed ligand complex species were done at concentration ratios T_M : T_{LP}: T_{LNA} = 1:1:1 (where M = Cu(II), Co(II), or Ni(II); P (peptide unit) = G, GG, GP, and GGG ligands; L_{NA} = NA ligand). The conductance readings were corrected by means of the equation:

$$\Omega_{corr}^{-1} = \Omega_{obs}^{-1}\left(\frac{V_1 + V_2}{V_1}\right) \tag{2}$$

assuming that the conductivity is a linear function of dilution, where Ω_{obs}^{-1} is the observed electrolytic conductivity, V_1 the initial volume of the titration cell and V_2 the volume of base added. The titration curves were plotted as corrected conductance against the volume of titrant used.

2.6 Cyclic Voltammetery Measurements

Cyclic voltammetric measurements were carried out using a computer controlled Autolab PGSTAT30 potentiostat (Eco-Chimie, Utrecht, Netherlands). All electrochemical

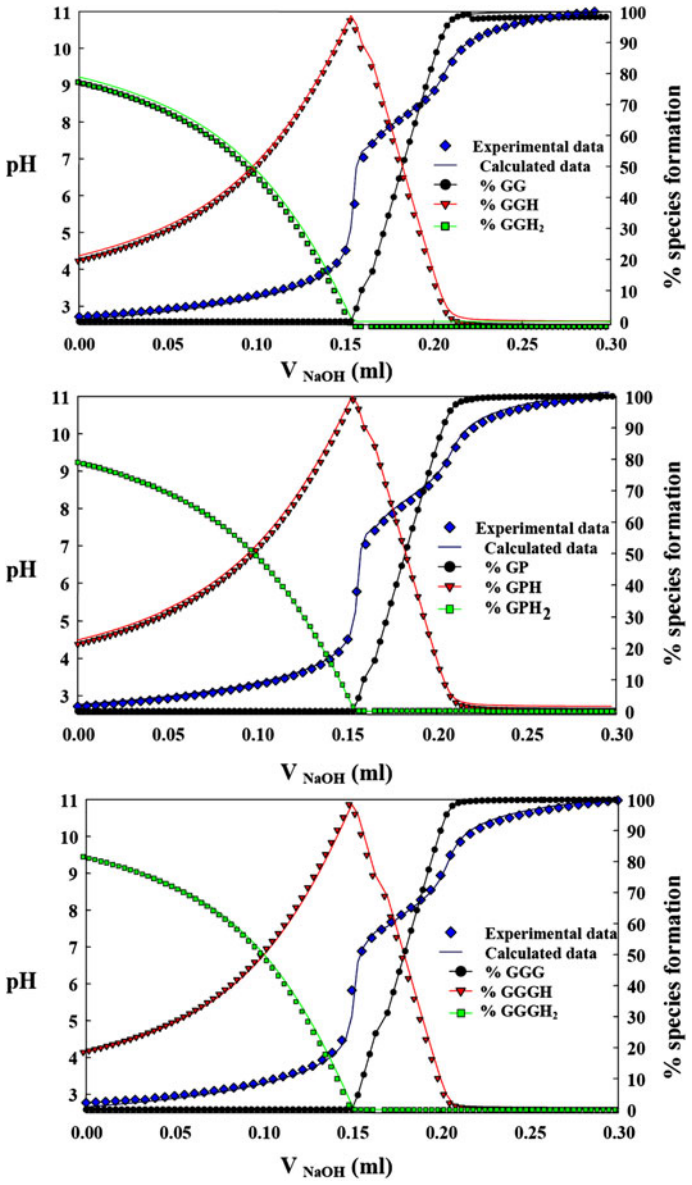

Fig. 1 Potentiometric titration curves and speciation diagrams of glycylglycine (GG), glycyl-L-phenylalanine (GP), and glycylglycylglycine (GGG) for protonation constants determination at 298.15 K and 0.15 mol·dm^{-3} $NaNO_3$

experiments were performed in a three-electrode airtight one compartment cell with a volume of 50 mL under an argon atmosphere. The three electrode system was comprised of (i) either a glassy carbon tip (GC) disc (3 mm diameter, Metrohm) or a platinum electrode disc (1.6 mm diameter, Metrohm) as a working electrode; (ii) an Ag/AgCl

electrode (1 mol·dm^{-3} KCl) was used as a reference electrode; and (iii) platinum wire served as the counter electrode. All measurements were carried out at room temperature (298 ± 0.1 K), with scan rate of 50 mV·sec^{-1} and an accuracy of ±1.0 mv. Prior to each measurement, the working electrode surface was cleaned by polishing with 0.25-μm diamond paste, followed by cleaning in ethanol and ultrapure water. Different electroactive metal complexes was prepared with concentration ratios T_M:T_L = 1:1 for binary complex species and ratios T_M:T_{Lp}:T_{LNA} = 1:1:1, (where M = Cu(II), Co(II), or Ni(II); P = G, GG, GP, and GGG ligands; L_{NA} = NA ligand, $T_M = T_{Lp} = T_{LNA}$ = 0.01 mol·dm^{-3}). General purpose electrochemistry system (GPES) software was used to display and interpret the data.

3 Result and Discussion

3.1 Protonation Equilibria of Vitamin B3 and G Peptides

The pH-potentiometric titration curves and speciation diagrams of G, GG, GP, and GGG are presented in Fig. 23 in Appendix 1 and in Fig. 1. The data analysis of the pH-potentiometric titration curves were refined with HYPERQUAD 2008, the protonation constants (pK_a) values of the ligands (NA, G, GG, GP, and GGG) were determined and are ported in Table 1 along with the some previous literature values [10, 28–39].

By comparing our calculated values (Table 1) with the literature values, we found a negligible variance, which could be explained by the differences in the experimental conditions. NA has an acid group and a basic group and the corresponding equilibria are shown is Scheme 1a, b [40].

The suggested stepwise acid dissociation processes of NA, G and its oligopeptides are shown in Scheme 2, where the protonation constants of NA are pKa_1 ~ 2.2314 and pKa_2 ~ 4.6246, resulting from the liberation of the protons of the carboxylic acid and pyridine nitrogen groups and the first deprotonation of the G peptides occurred at the carboxyl group of C-terminus, followed by deprotonation of the amine group of the N-terminus.

Table 1 Protonation constants of nicotinic acid and glycine peptides in water at 298.15 K and 0.15 mol·dm^{-3} $NaNO_3$

Ligands	pK_{a1}	pK_{a2}
Nicotinic acid	2.2314 ± 0.0073 (2.33)[a]	4.6246 ± 0.0211 (2.33)[a]
Glycine	2.4134 ± 0.0077 (2.33)[b]	9.7101 ± 0.0055 (9.61)[b]
Glycylglycine	3.2713 ± 0.0045 (3.16)[c]	8.1971 ± 0.0061 (8.15)[c]
Glycyl-L-phenylalanine	3.3324 ± 0.0144 (3.23)[d]	7.9941 ± 0.0123 (8.11)[d]
Glycylglycylglycine	3.3134 ± 0.0112 (3.26)[e]	7.6347 ± 0.0074 (7.93)[e]

[a] Ref. [15], T = 298.15 K, I = 0.1 mol·dm^{-3} $NaNO_3$

[b] Ref. [28], T = 298.15 K, I = 0.05 mol·dm^{-3} KCl

[c] Ref. [29], T = 298.15 K, I = 0.1 mol·dm^{-3} KNO_3

[d] Ref. [38], T = 298.15 K, I = 0.1 mol·dm^{-3} $NaClO_4$

[e] Ref. [30], T = 298.15 K, I = 0.1 mol·dm^{-3} KNO_3

3.2 Complex Formation Equilibria of Vitamin B3 and G Peptides

Representative pH-potentiometric titration curves for the binary and mixed ligand complexes involving copper(II), cobalt(II), and nickel(II) ions, and NA with G peptides are shown in Figs. 2 and 3. The protonation constants of the ligands were used, in conjunction with the pH titration data, in the determination of the stability constants of the complexes

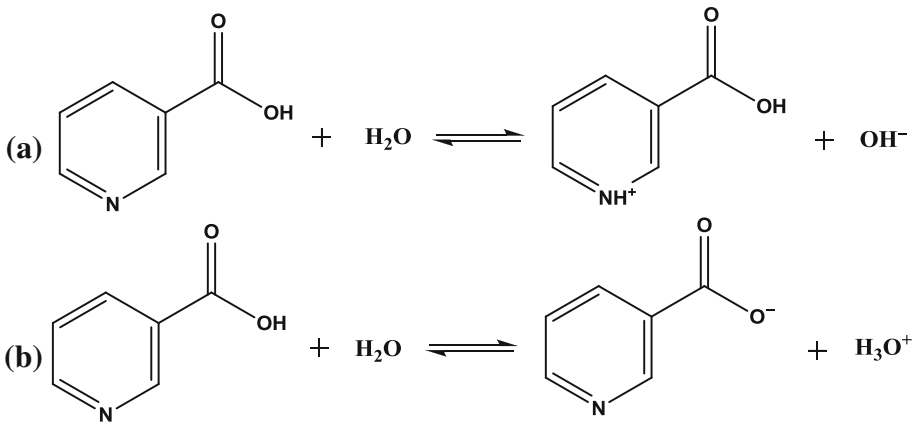

Scheme 1 Nicotinic acid equilibrium when acting as: **a** base, **b** acid

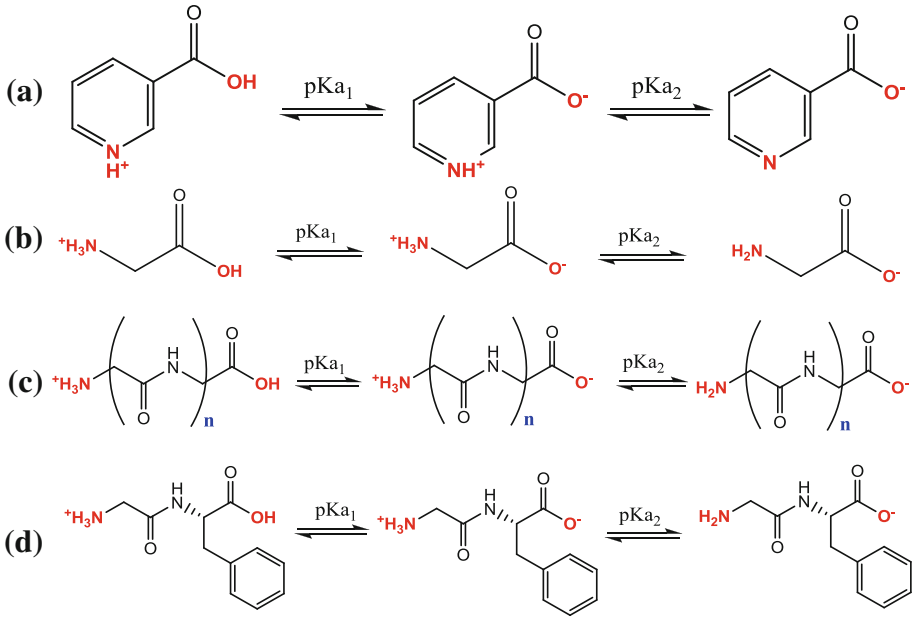

Scheme 2 Protonation equilibria of **a** nicotinic acid, **b** glycine, **c** glycine small peptide; $n = 1$ for glycylglycine (GG), $n = 2$ for glycylglycylglycine (GGG) and **d** glycyl-L-phenylalanine

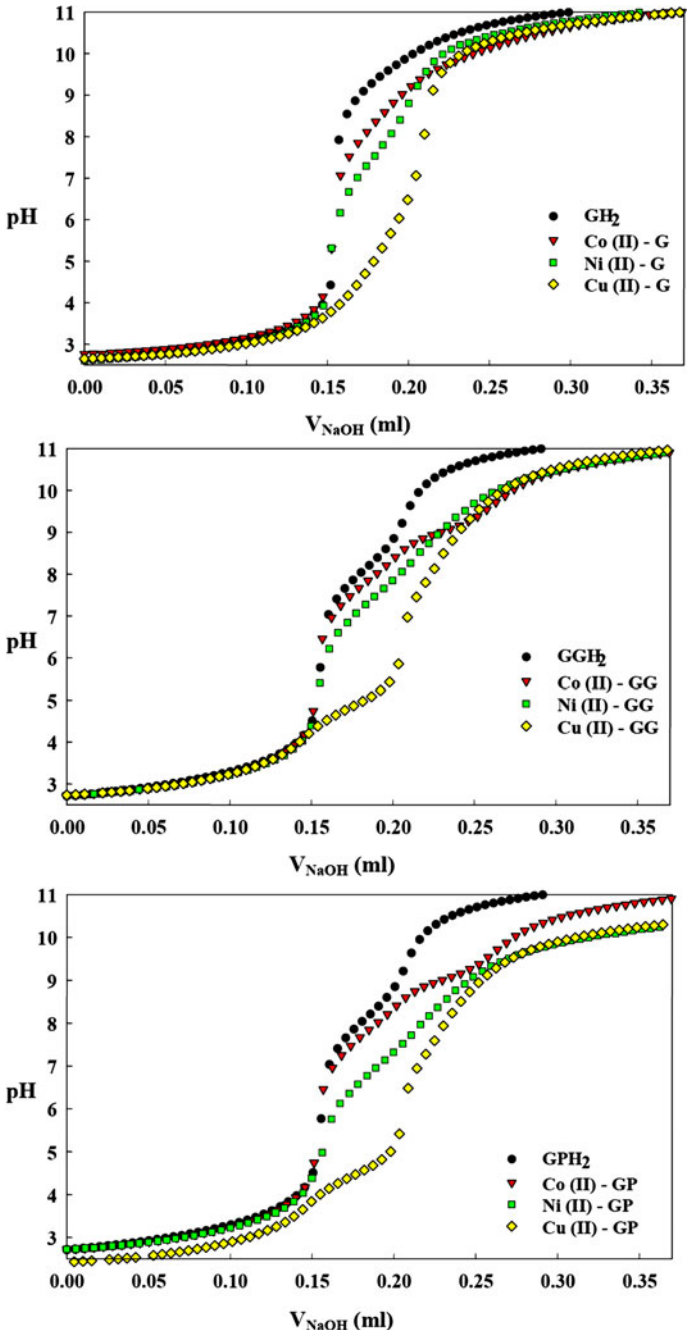

Fig. 2 Experimental potentiometric titration curves of glycine (G), glycylglycine (GG), and glycyl-L-phenylalanine (GP) binary metal complexes at 298.15 K and 0.15 mol·dm^{-3} $NaNO_3$

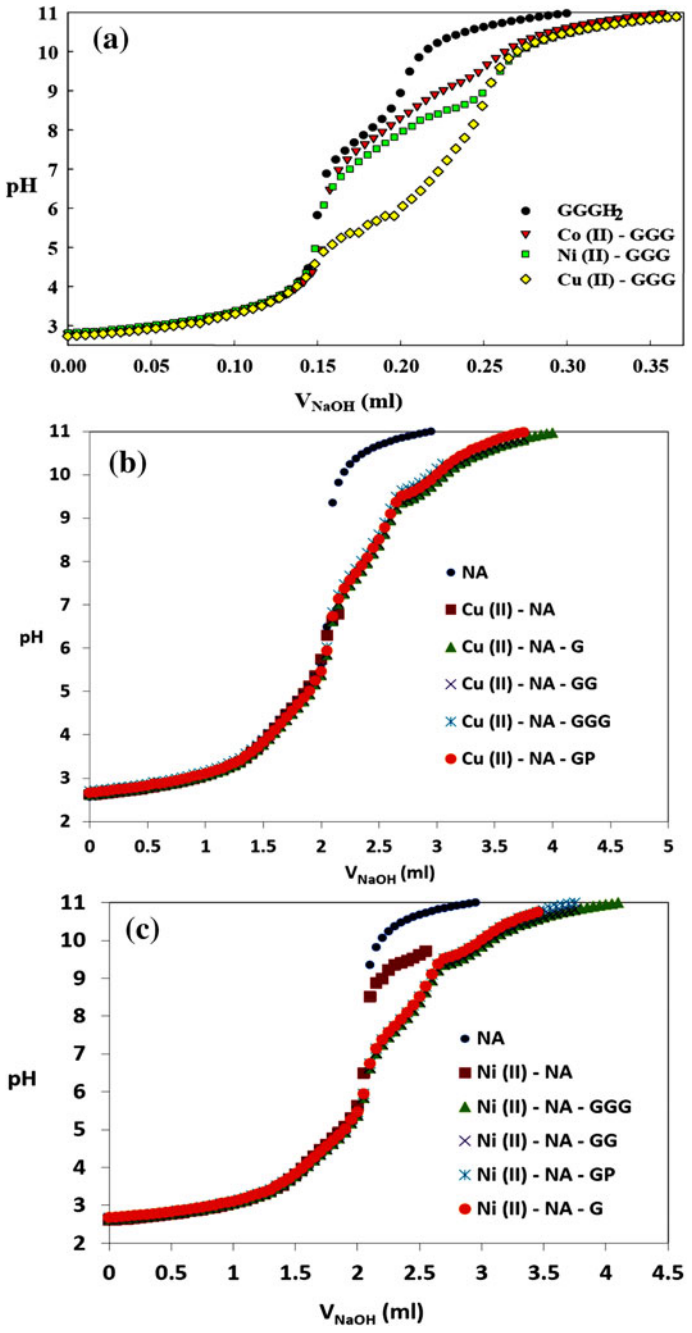

Fig. 3 Experimental potentiometric titration curves of **a** glycylglycylglycine binary metal complexes, **b** binary and mixed ligand Cu(II) complexes and **c** binary and mixed ligand Ni(II) complexes at 298.15 K and 0.15 mol·dm^{-3} $NaNO_3$

Table 2 Overall formation constants ($\log_{10} \beta_{pqrs}$) of Cu(II), Ni(II), and Co(II)–nicotinic acid (NA) and glycine peptide complexes

Species	$\log_{10} \beta_{pqrs} \pm$ S.D.					
	Cu(II)		Ni(II)		Co(II)	
NA = Nicotinic acid						
MNA^+	3.3104 ± 0.0105	(3.23)[a]	2.6978 ± 0.0241	(2.66)[a]	Not determined	
MNAOH	−2.3124 ± 0.0234				Not determined	
G = Glycine						
$[MG]^+$	8.2728 ± 0.0175	(8.22)[b]	5.6774 ± 0.0238	(5.80)[b]	5.1113 ± 0.0163	(5.07)[e]
$[MG_2]$	15.3438 ± 0.0141	(15.11)[b]	10.5041 ± 0.1065	(10.65)[b]	8.1497 ± 0.0574	(9.04)[b]
$[MG_3]^-$	19.6155 ± 0.0334		14.8895 ± 0.0210			
$[MGH_{-1}]$	1.3028 ± 0.0116		−3.2119 ± 0.0242		−4.2119 ± 0.0451	
$[MGH_{-2}]^-$	−9.1725 ± 0.0205		−13.6151 ± 0.0346		−13.8474 ± 0.0248	
GG = Glycylglycine						
$[MGG]^+$	5.5460 ± 0.0527	(5.68)[c]	4.2733 ± 0.0423	(4.11)[d]	3.7362 ± 0.0063	
$[MGGH_{-1}]$	1.4758 ± 0.0104	(1.50)[c]	7.4755 ± 0.0794	(7.32)[d]	−5.1819 ± 0.0100	
$[MGGH_{-2}]^-$	−7.4318 ± 0.0121		−3.7066 ± 0.0287		Not determined	
GP = Glycyl-L-phenylalanine						
$[MGP]^+$	7.6573 ± 0.0337		4.9874 ± 0.0343		3.6278 ± 0.0174	
$[MGPH_{-1}]$	3.7324 ± 0.0153		7.7341 ± 0.0703		1.2119 ± 0.0153	
$[MGPH_{-2}]^-$	−3.4745 ± 0.0091		−3.3461 ± 0.0207		Not determined	
GGG = Glycylglycylglycine						
$[MGGG]^+$	5.1234 ± 0.0223	(5.24)[d]	4.2105 ± 0.0212		3.5462 ± 0.0194	
$[MGGGH_{-1}]$	0.0901 ± 0.0099	(0.02)[d]	7.3226 ± 0.0857		−5.3911 ± 0.0693	
$[MGGGH_{-2}]^-$	−6.7152 ± 0.0109	(−6.58)[d]	−4.3427 ± 0.0612		−13.9464 ± 0.0477	

All the values were calculated with the program HYPERQUAD 2008 from potentiometric investigations at ca. 298 K and $I = 0.15$ mol·dm^{-3} $NaNO_3$. The symbols p, q, r, and s are used to indicate the stoichiometric coefficients associated with the possible equilibria in solutions

[a] Ref. [15], $T = 298.15$ K, $I = 0.1$ mol·dm^{-3} $NaNO_3$

[b] Ref. [28], $T = 298.15$ K, $I = 0.05$ mol·dm^{-3} KCl

[c] Ref. [29], $T = 298.15$ K, $I = 0.1$ mol·dm^{-3} KNO_3

[d] Ref. [30], $T = 298.15$ K, $I = 0.1$ mol·dm^{-3} KNO_3

of the Cu(II), Ni(II), Co(II)) ions with NA, G and the G peptides using HYPERQUAD 2008.

Stability of the various metal complexes formed in 0.15 mol·dm^{-3} $NaNO_3$ solutions are expressed as overall formation constants β_{pqrs} and are reported in Table 2 as $\log_{10} \beta_{pqrs}$.

Among the metal ions studied, Cu(II) formed the most stable complexes with G peptides or NA, followed by Ni(II) and Co(II). This tendency was found for all of the G peptides and is in good agreement with the Irving–Williams series [31] that is mainly dependent on the metal ionic radius, crystal field stabilization energy and Jahn–Teller distortion. For each metal ion studied, G formed the most stable complex species, followed by the GG, GP and GGG metal complexes, and then by NA metal complexes. As a bridging ligand, NA has been used to bridge nickel(II) ion in two different coordination modes. The first mode is a bridging mode where each ligand bridges two metal atoms (Scheme 3I) and the second mode is the terminal

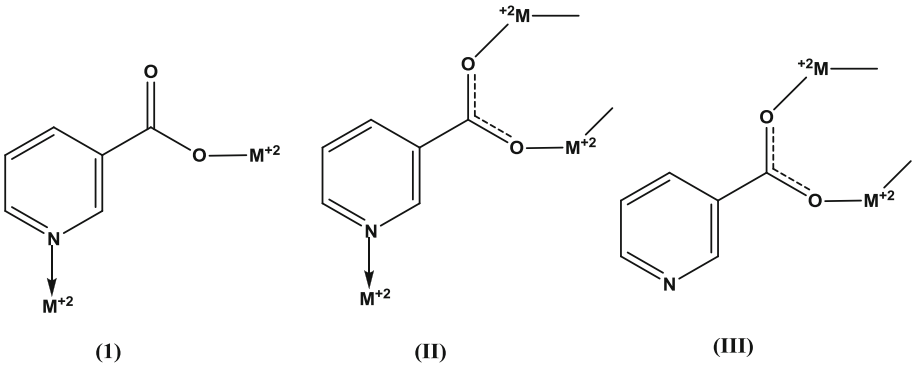

Scheme 3 Possible bridging of nicotinic acid to metal ions

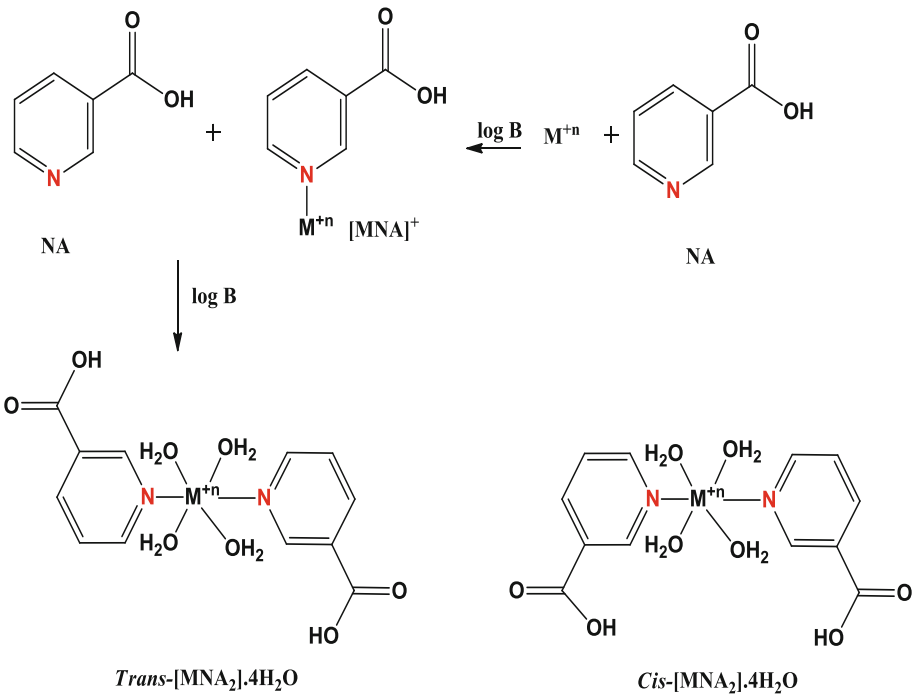

Scheme 4 Proposed metal ion binary ligand complex formation equilibria involving nicotinic acid

mode, where it is bonded to one metal atom only by one of its two carboxyl oxygen atoms (Scheme 3II) [41]. The behavior of NA as monodentate ligand was observed in the case of divalent copper complexes (Scheme 3I).

An infrared study of NA complexes with divalent copper revealed that the carboxyl group of NA remains unchanged which indicates that there is no metal-to-oxygen coordination in this complex. Furthermore, the complex shows appreciable changes in the pyridine part of the NA spectrum [42]. It has been proposed that this monodentate behavior of NA explains the biological activity and glucose tolerances of Cr(III) and some divalent

metal ions coordinated to NA [43]. The authors found that only trivalent Cr(III) was coordinated to the carboxyl oxygen of NA while the other metal ions were coordinated to the pyridine nitrogen of NA. This interesting phenomenon can be explained according to the theory of hard and soft acids and bases (HSAB) [44]. Trivalent chromium ion is a hard base so it has preference to coordinate with the carboxyl oxygen, which is a hard acid, instead of the pyridine nitrogen. On the other hand, all the divalent metal ions that they studied were soft bases and so they will coordinate with the pyridine nitrogen of NA. Another report stated that NA may also act as a neutral ligand, ligating the metal ion through its N atom, as found in its copper(I) and gold(III) complexes, or as the nicotinate anion that forms complexes with lanthanides by two carboxylate O atoms forming a four member chelate ring, thus acting as a bidentate ligand [44]. The reasonable complex formation equilibria processes of NA, G and its peptides are illustrated in Schemes 4, 5, 6, 7 and 8.

The protonation constants of the ligands and the overall stability constants of the binary NA, G, GG, GP, and GGG complexes with Cu(II), Co(II) and Ni(II) metal ions were determined in the present work and compared with values from the literature [28–39]. They were used as input for the determination of the mixed-ligand complex species stability

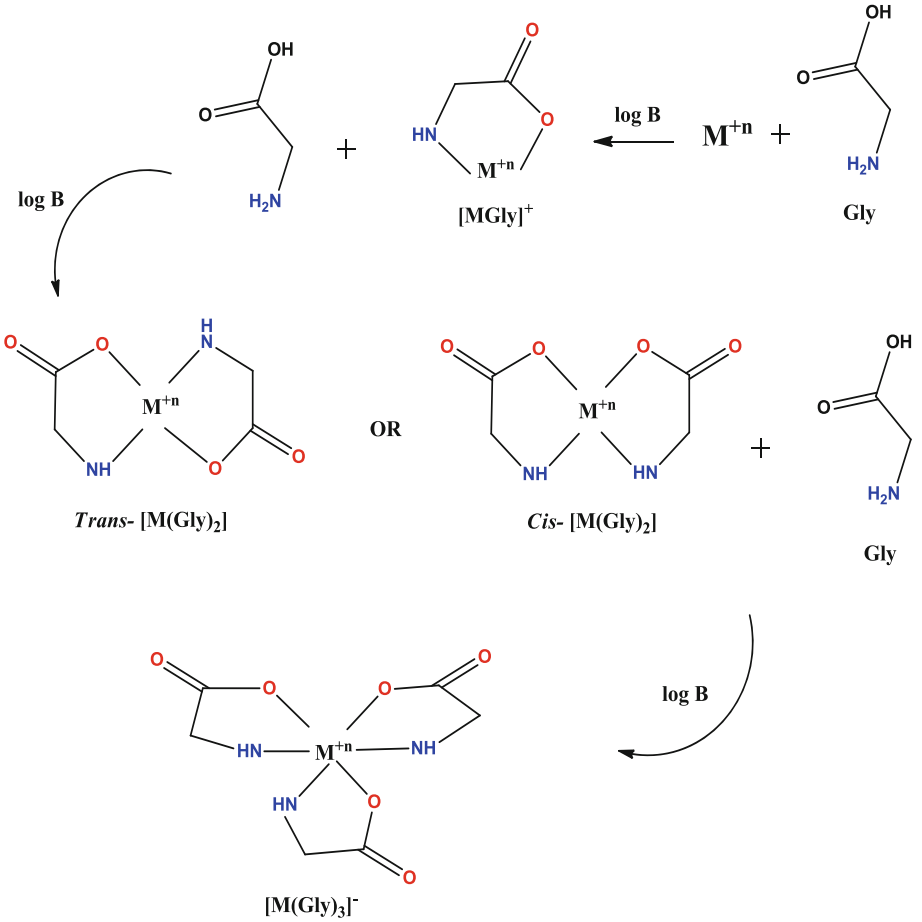

Scheme 5 Proposed metal ion binary ligand complex formation equilibria involving glycine

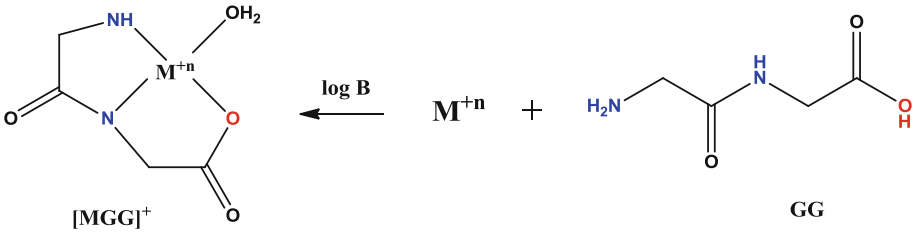

Scheme 6 Proposed metal ion binary ligand complex formation equilibria involving glycylglycine

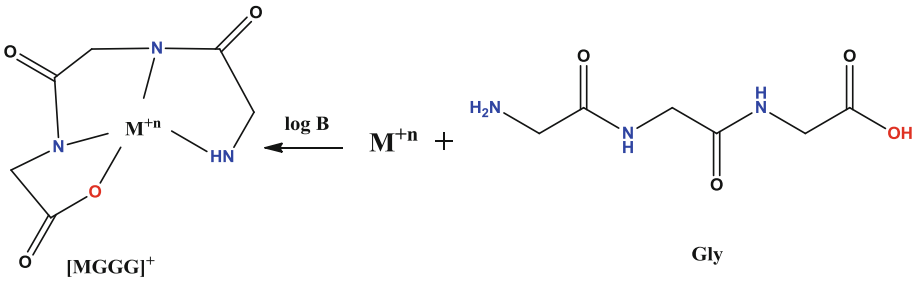

Scheme 7 Proposed metal ion binary ligand complex formation equilibria involving glycylglycylglycine

constants which are reported in Table 3. With regard to the metal ions, the trend observed matched the Irving–William series [31] with the most and the least stable complexes being with copper and cobalt, respectively, for all ligands (Scheme 9).

From the global protonation and complex species stability constants, distribution diagrams of various complex species formed in the 0.15 mol·dm^{-3} $NaNO_3$ solution were generated using the HYSS2009 program. Representative complex species distribution diagrams of Cu(II), and Ni(II) binary and mixed ligand complexes are supplied in Figs. 4 and 5, based on the data in Tables 1, 2 and 3. These diagrams clearly show that complexes are formed in certain pH ranges. For systems containing NA, since NA form slightly less stable complexes with metal ions compared to the G peptides, the competition between NA and different G peptides can be seen in the complex species distribution diagrams where at approximately pH = 6, the $[CuNA]^+$, and $[NiNA]^+$ complexes are formed at nearly the same amount, 53 and 38 %, respectively. Figures 4 and 5 show the distributions of two different binary and mixed ligand complex species: (i) the first are the protonated complexes that involve $[MGH_{-1}]$, $[MGH_{-2}]^-$, $[MGGH_{-1}]$, $[MGGH_{-2}]^-$, $[MGPH_{-1}]$, $[MGPH_{-2}]^-$, $[MGGGH_{-1}]$, $[MGGGH_{-2}]$ and, for binary complex species $[MNAGH_2]^-$, $[MNAGH]^{2-}$, $[MNAGGH_2]^-$, $[MNAGGH]^{2-}$, $[MNAGGH_{-1}]^{4-}$, $[MNAGPH_2]^-$, $[MNAGPH]^{2-}$, $[MNAGPH_{-1}]^{4-}$, $[MNAGGGH_2]^-$, $[MNAGGGH]^{2-}$, $[MNAGGGH_{-1}]^{4-}$ for mixed ligand complex; (ii) the second complex species are deprotonated complexes ($[MNA]^+$, $[MG]^+$, $[MG_2]$, $[MG_3]^-$, $[MGG]^+$, $[MGP]^+$, $[MGGG]^+$) for binary species and ($[MNAG]^{3-}$, $[MNAGG]^{3-}$, $[MNAGP]^{3-}$, $[MNAGGG]^{3-}$ for mixed ligand complex species. From the diagrams in Figs. 4 and 5, it can be seen that almost all protonated complex species (MA_xH_x) start to form at low pH ($\leq$7). It is because under this condition, the ligand

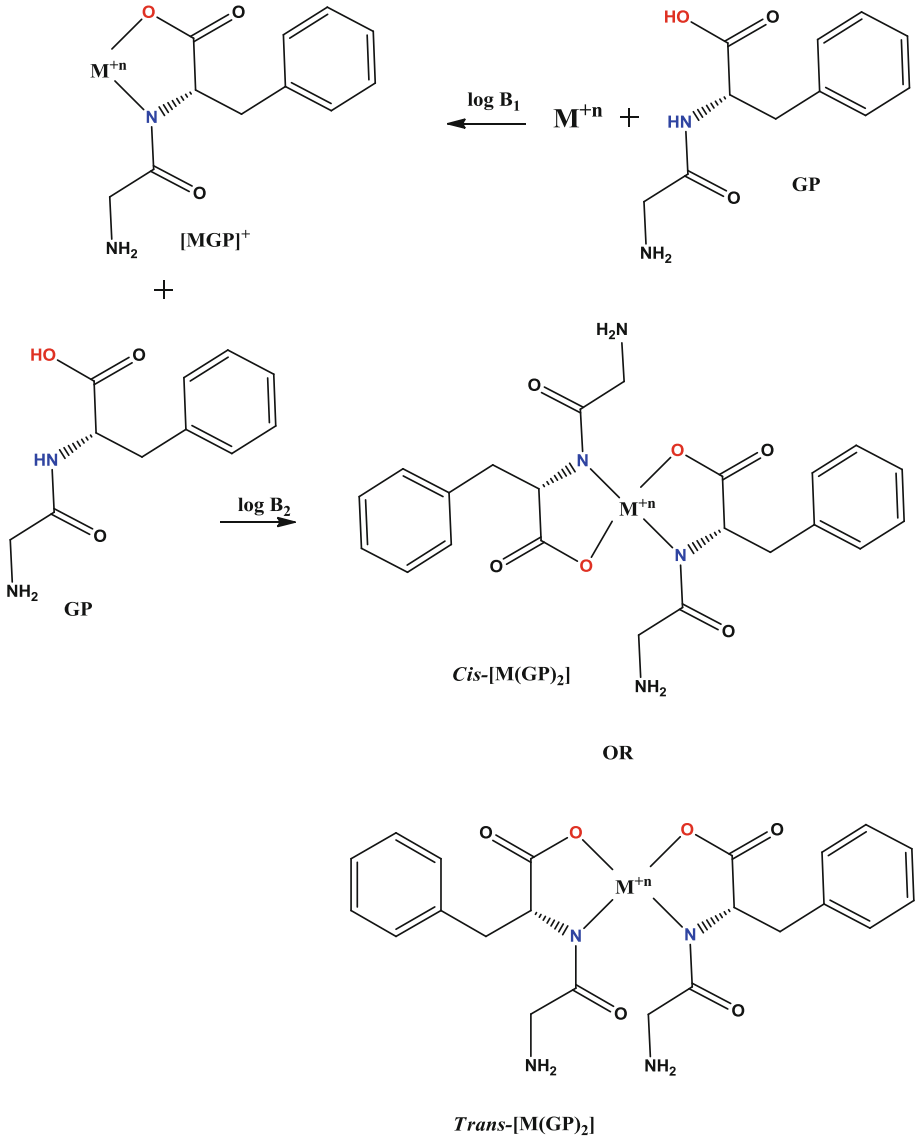

Scheme 8 Proposed metal ion binary ligand complex formation equilibria involving glycyl-L-phenylalanine

occurs in various protonated forms. On the other hand, deprotonated complexes of are formed first at slightly higher pHs.

The influence of the peptide bond in the G oligopeptides (M = Cu(II), Co(II), and Ni(II); P = G, GG, GGG, and GP) in its undeprotonated and deprotonated forms are compared and investigated in the following expressions:

$$M + P \rightleftharpoons MP\,, \quad [MP] = \beta_{MP}[M]\,[P] \tag{3}$$

Table 3 Overall formation constants ($\log_{10} \beta_{pqrs}$) of divalent metal ions Cu(II), Ni(II), and Co(II)–nicotinic acid (NA)–glycine peptide (G, GG, GP, GGG) complexes

Species	$\log_{10} \beta_{pqrs} \pm$ S.D.		
	Cu(II)	Ni(II)	Co(II)
G = Glycine			
$[MNAGH_2]^-$	38.3434 ± 0.0330	34.0021 ± 0.0151	Not determined
$[MNAGH]^{2-}$	32.3941 ± 0.0252	25.5970 ± 0.0123	Not determined
$[MNAG]^{3-}$	22.2458 ± 0.0321	15.2826 ± 0.0173	Not determined
GG = Glycylglycine			
$[MNAGGH_2]^-$	37.4138 ± 0.0211	Not determined	Not determined
$[MNAGGH]^{2-}$	31.2003 ± 0.0452	24.5752 ± 0.0167	Not determined
$[MNAGG]^{3-}$	22.5739 ± 0.0407	14.7319 ± 0.0203	Not determined
$[MNAGGH_{-1}]^{4-}$	Not determined	3.6423 ± 0.0503	Not determined
GP = Glycyl-L-phenylalanine			
$[MNAGPH_2]^-$	37.4008 ± 0.0281	28.6463 ± 0.0143	Not determined
$[MNAGPH]^{2-}$	31.1113 ± 0.0352	24.5352 ± 0.0171	Not determined
$[MNAGP]^{3-}$	22.7169 ± 0.0547	14.8073 ± 0.0203	Not determined
$[MNAGPH_{-1}]^{4-}$	Not determined	3.2822 ± 0.0503	Not determined
GGG = Glycylglycylglycine			
$[MNAGGGH_2]^-$	35.9804 ± 0.0403	Not determined	Not determined
$[MNAGGGH]^{2-}$	30.6043 ± 0.0247	24.2685 ± 0.0272	Not determined
$[MNAGGG]^{3-}$	22.3816 ± 0.0476	15.0841 ± 0.0482	Not determined
$[MNAGGGH_{-1}]^{4-}$	Not determined	3.1492 ± 0.03221	Not determined

All the values were calculated with the program HYPERQUAD 2008 from potentiometric investigations at 298 K and $I = 0.15$ mol·dm^{-3} $NaNO_3$. The symbols p, q, r, and s are used to indicate the stoichiometric coefficients associated with the possible equilibria in solutions

$$M + P \rightleftharpoons MPH_{-1} + H \qquad [MPH_{-1}] = \beta_{MPH-1}[M][P]/[H] \tag{4}$$

$$M + P \rightleftharpoons MPH_{-2} + 2H \qquad [MPH_{-2}] = \beta_{MPH-2}[M][P]/[H]^2 \tag{5}$$

$$MP \rightleftharpoons MPH_{-1} + H \qquad [MPH_{-1}] = K_{MPH-1}[MP]/[H] \tag{6}$$

$$\beta_{MPH-1} = K_{MPH-1}\beta_{MP} \tag{7}$$

$$MP \rightleftharpoons MPH_{-2} + 2H \qquad [MPH_{-2}] = \beta_{MPH-2}[MP]/[H] \tag{8}$$

$$\beta_{MPH-2} = K_{MPH-2}\beta_{MP} \tag{9}$$

where in G metal complexes, a negative stoichiometric value for H refers to the hydroxy complex, while in case of G oligopeptides (GG, GP and GGG) metal complexes it refers to the deprotonation of the amide nitrogen in the peptide bond. For example, the MPH_{-1} in the system containing GG or GP refers to the formation of the complex between a metal ion with this ligand in its amide deprotonated form (GGH_{-1}, or GPH_{-1}). Subtraction of $\log_{10} \beta_{MP}$ of G from those of GG, GP and GGG ligands as well as subtraction of $\log_{10} \beta_{MP}$ of GG, and GP from that of GGG were carried out to evaluate the effect of undeprotonated amide nitrogen peptide bonds. The negative $\log_{10} \beta_{MP}$ values indicate the absence of an undeprotonated amide nitrogen contribution in the complexation of metal ions with G oligopeptides (G, GG, GP and GGG) ligands. It is interesting to note that the $\Delta\log_{10} \beta_{MP}$

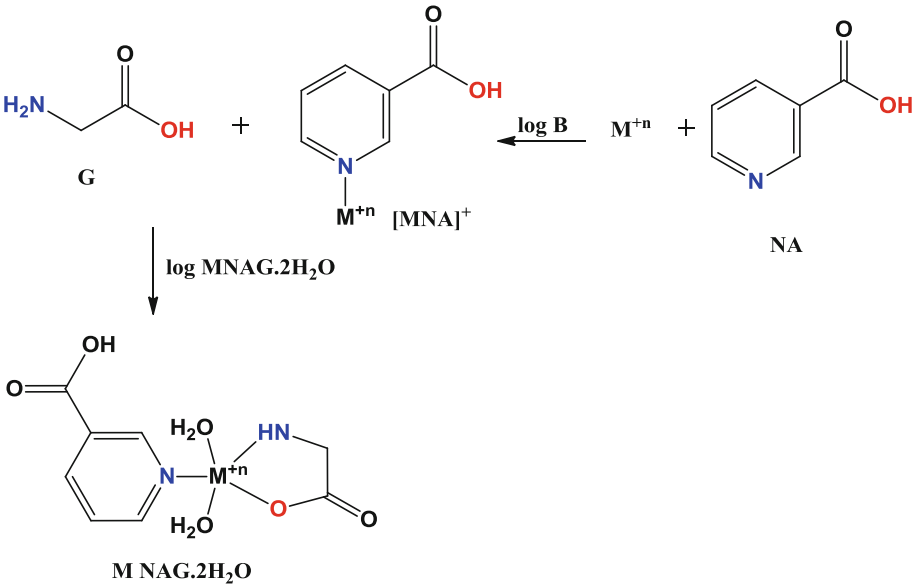

Scheme 9 Proposed metal ion mixed ligand complex formation equilibria involving nicotinic acid and glycine peptide unit

values of metal complexes involving GG, GP and GGG are very small (between −0.08 to −0.26) while subtracted values of the $\log_{10}\beta_{MP}$ of GG-G, GP-G and GGG-G vary from −1.34 to −2.92. This interesting phenomenon can be explained from the structure of the peptide ligands itself. G, the smallest and the simplest ligand, can form a five-membered ring complex with metal ion via deprotonated amine and carboxyl groups of the amino acid, while for the GG and GGG, the metal ions will form complexes with the deprotonated amine group in the N-terminus and form a less stable chelate with the peptide oxygen. The small $\Delta\log_{10}\beta_{MP}$ values of G oligopeptides (GGG-GG, GGG-GP) occur due to the extensive backbone length of GGG as a ligand leading to the occurrence of steric effects. Since GG and GGG form chelates in the same manner, the stabilities of the complexes formed are similar. On the other hand, the calculated $\Delta\log_{10}K_{MPH-1}$ and $\Delta\log_{10}K_{MPH-2}$ values were found to be positive indicating that the deprotonated amide nitrogen participates in the complexation of the metal ions. $\Delta\log_{10}K_{MPH-2}$ is more positive than $\Delta\log_{10}K_{MPH-1}$ due to the contribution of two deprotonated amides in GGG where the metal ions and GGG form three five-membered chelate rings, while in the metal ion GG/GP systems the complex forms two five-membered chelate rings via nitrogen in the N-terminus, and deprotonated amide nitrogen of the peptide and carboxyl in the C-terminus. It can also be seen that the contributions of peptide amide are also affected by Pearson's HSAB rule [45]; since the amide group is classified as a borderline base, this binding site has a greater influence on the borderline bases Cu(II), Ni(II) and Co(II).

3.3 Gaussian Molecular Modeling

In addition to geometry optimization, frequency analysis of complexes between one metal and one ligand were carried out. The Gibbs energy (G) that was obtained from output of

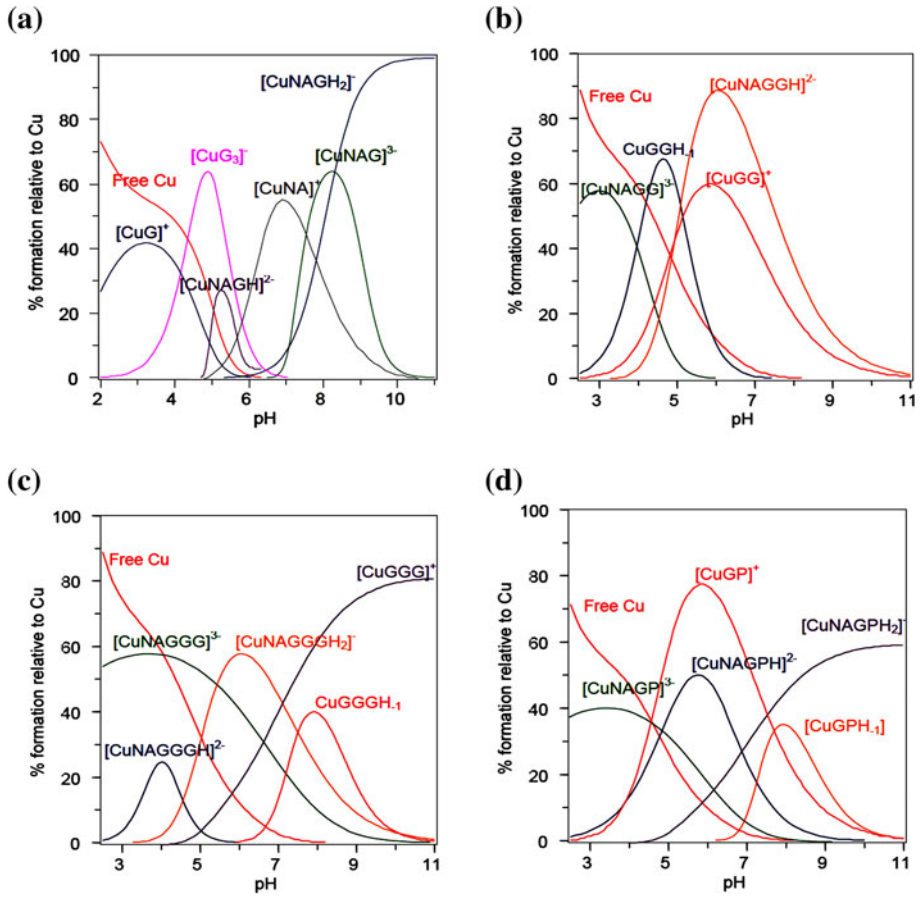

Fig. 4 The species distribution curves for the complex species of **a** the Cu(II)–nicotinic acid (NA)–glycine (G) systems, **b** the Cu(II)–nicotinic acid (NA)–glycylglycine (GG) systems, **c** the Cu(II) + nicotinic acid (NA)–glycylglycylglycine (GGG) systems and **d** the Cu(II) + nicotinic acid (NA)–glycyl-L-phenylalanine (GP) system. Percentages are calculated with respect to the analytical concentration of the metal ion

frequency analysis then was used to verify the contributing binding site of the ligands and to predict the structure of the complexes by the following equation:

$$\begin{aligned} M^{2+} + L^{-} &\rightleftharpoons [ML]^{+} \\ \Delta_r G &= \Sigma G_{\text{product}} - \Sigma G_{\text{reactant}} \end{aligned} \tag{10}$$

$$\Delta_r G = G_{[ML]} - (G_M + G_L) \tag{10a}$$

where the Gibbs energy of reaction ($\Delta_r G$) is proportional to the metal complex formation constant ($\log_{10}\beta$). Thus, according to this correlation, the more negative the $\Delta_r G$ value is, the larger the formation constant value will be and the complex that is formed will be more stable. For each metal–ligand combination, Gaussian modelings were done by considering the possible binding sites that could contribute to complex formation. The Gibbs energy of reaction ($\Delta_r G$) for metal ligand formation with their possible binding site of ligands were

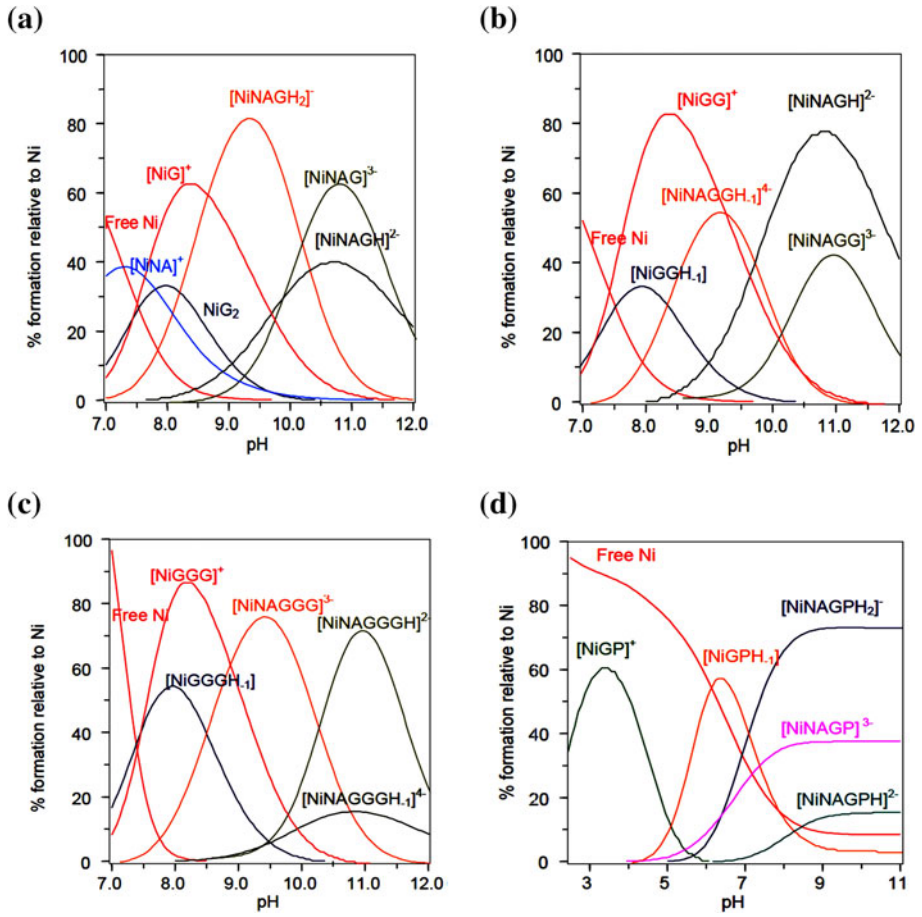

Fig. 5 The species distribution curves for the complex species of **a** the Ni(II)–nicotinic acid (NA)–glycine (G) systems, **b** the Ni(II)–nicotinic acid (NA)–glycylglycine (GG) systems, **c** the Ni(II) + nicotinic acid (NA)–glycylglycylglycine (GGG) systems and **d** the Ni(II) + nicotinic acid (NA)–glycyl-L-phenylalanine (GP) system. Percentages are calculated with respect to the analytical concentration of the metal ion

calculated and the ones which showed the most negative value of $\Delta_r G$ (Table 4) were chosen as possible contributing binding sites, and the structure of these complexes were assumed to be the structures of the complexes formed. By looking to the data in Table 4, for instance in the case of copper(II)–G complexes, G may complex with the metal ion through its amine group and carboxyl group so during Gaussian geometry optimization and frequency calculations, the calculations were done with the metal ion bound to G through its amine group only, carboxyl group only and with chelate binding through the amine and carboxyl groups. The values of these $\Delta_r G$ shows that G complexes with Cu(II) through its amine and carboxyl groups and acts as a bidentate chelating ligand. Similarly, NA, GG, GP, and GGG formed chelates through their nitrogen and oxygen atoms. In agreement with the Hyperquad refined results, it seems that the G and GP have more negative $\Delta_r G$ values compared to the other ligands. This phenomenon might be because of formation of three and two stable five-membered ring metal complexes with G and GP, while other ligands

Table 4 Gibbs energy of reaction for complexes obtained from optimization and frequency calculations using Gaussian 09

Molecule	G (Hartree/particle)[a]	$\Delta_r G$ (kJ·mol^{-1})
Metal ions		
Cu2+	−1,639.813789	
Ni2+	−1,507.725005	
Co2+	−1,382.251038	
Ligands		
NA	−436.375509	
G	−283.956410	
GG	−491.941243	
GP	−523.734591	
GGG	−699.922905	
Cu(II) complexes		
$[CuNA]^+$	−2,076.365366	−462
[CuG]	−1,923.995847	−619
CuGG	−2,131.948785	−509
CuGP	−1,987.876943	−615
CuGGG	−2,339.923634	−491
Ni(II) complexes		
$[NiNA]^+$	−1,994.205740	−276
NiG	−1,791.859317	−467
NiGG	−1,999.812184	−383
NiGP	−1,876.321946	−511
NiGGG	−2,207.789795	−373
Co(II) complexes		
[CoNA]	Not determined	Not determined
CoG	−1,666.343510	−357
CoGG	−1,874.301105	−286
CoGP	−1,732.326545	−3,760
CoGGG	−2,082.272667	−259
M-NA-P complexes		
CuNAG	−1,912.653214	−533
CuNAGG	−2,032.231587	−492
CuNAGP	−1,834.852943	−560
CuNAGGG	−2,164.645319	−458
NiNAG	−1,804.364120	−420
NiNAGG	−1,832.364251	−352
NiNAGP	−1,764.328510	−481
NiNAGGG	−2,132.345912	−342

[a] The calculation was done using density functional theory (DFT)-B3LYP method combined with 6-31 + G(d) a basis set; 1 Hartree/particle = 2.6255048×10^3 kJ·mol^{-1}

form less stable five-membered ring complexes; in addition GP has a bulkier side chain. On the other hand, compared to GG and GGG which are bulky, G and GP have been shown to form more stable complexes with metal ions.

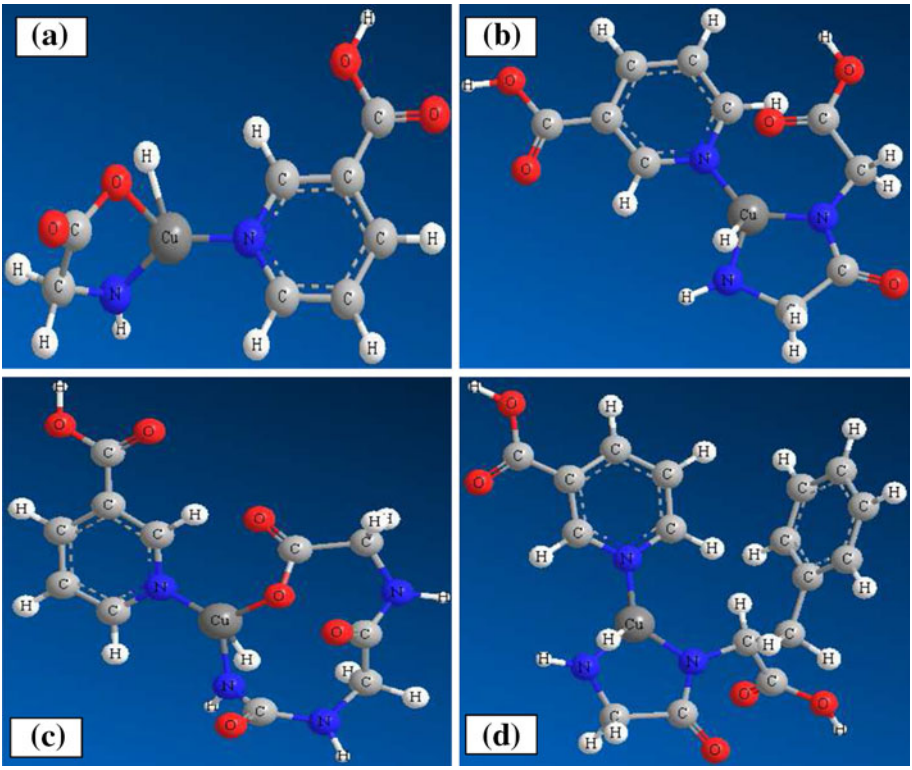

Fig. 6 Optimized structures of some mixed ligand complexes between divalent metal ion (Cu(II))–nicotinic acid–glycine contained peptides **a** CuNAG, **b** CuNAGG, **c** CuNAGP and **d** CuNAGGG; generated from Gaussian09 calculations

In addition, the Gaussian modeling of complexes between metal ions and peptides with deprotonated amide bonds were carried out. From the calculated value of $\Delta_r G$ in Table 4, the $\Delta_r G$ and complex stability decrease in the following order: $[MGGGH_{-2}]^- > [MGGH_{-1}] > [MGGGH_{-1}] > [MG]^+ > [MGG]^+ \geq [MGP]^+ \geq [MGGG]^+$. The optimized geometry of copper –NA–G peptide units, shown in Fig. 6, and the calculated values of $\Delta_r G$ support the hypothesis that the deprotonated amide in the GGG peptide forms three five-membered chelate rings with the metal ions while in metal ion–GG systems the complex forms two five-membered chelate rings via the N-terminus nitrogen, and the deprotonated amide nitrogen of peptide and C-terminus carboxyl.

3.4 UV–Vis Spectra Analysis

To confirm the complex formation equilibria in each system, UV–Vis spectrophotometric measurements were performed in the range 340–800 nm. By comparing the maximum absorption wavelength, the shapes of the absorption curves of each complexes, the shifting peaks and/or the new peaks that occur in the spectra, it was possible to observe complex formation in each system (Figs. 7, 8, 9, 10, 11, 12, 13, 14, 15, 16, 17, 18). The measurements demonstrated that the ligands NA, G, GG, GP, and GGG have one maximum

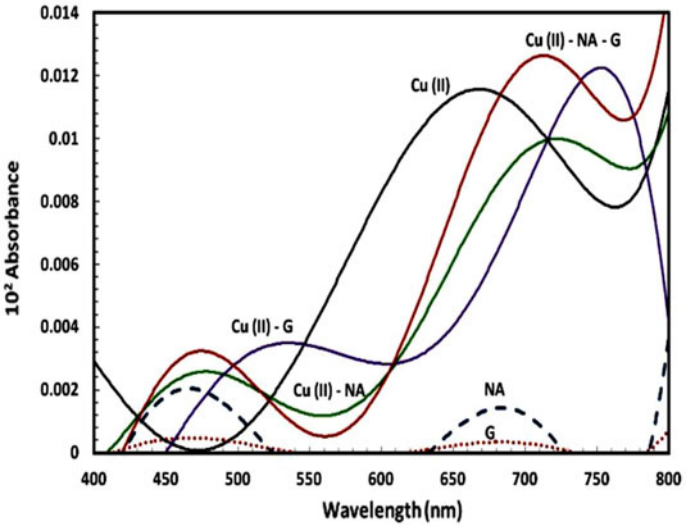

Fig. 7 Absorption spectra for (NA) nicotinic acid, (G) glycine, (Cu(II)–NA) binary system (0.001 mol·dm^{-3} Cu(II) + 0.001 mol·dm^{-3} nicotinic acid); (Cu(II)–G) binary system (0.001 mol·dm^{-3} Cu(II) + 0.001 mol·dm^{-3} glycine); (Cu(II)–NA–G) ternary system (0.001 mol·dm^{-3} Cu(II) + 0.001 mol·dm^{-3} nicotinic acid + 0.001 mol·dm^{-3} glycine)

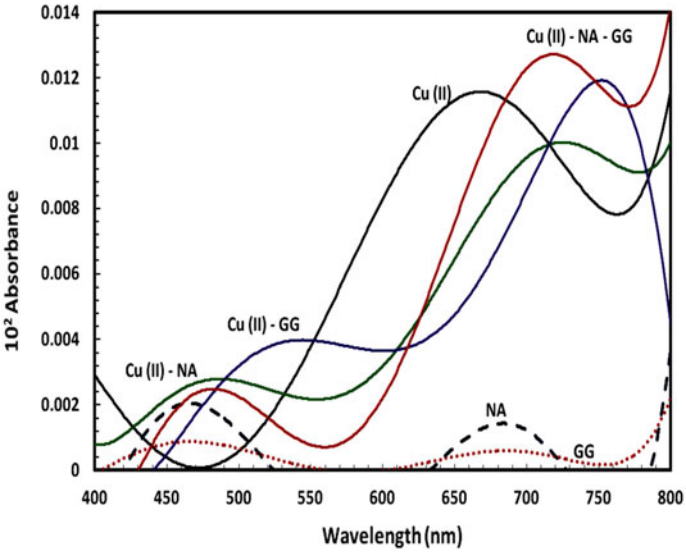

Fig. 8 Absorption spectra for (NA) nicotinic acid, (GG) glycylglycine, (Cu(II)–NA) binary system (0.001 mol·dm^{-3} Cu(II) + 0.001 mol·dm^{-3} nicotinic acid); (Cu(II)–GG) binary system (0.001 mol·dm^{-3} Cu(II) + 0.001 mol·dm^{-3} glycylglycine); (Cu(II)–NA–GG) ternary system (0.001 mol·dm^{-3} Cu(II) + 0.001 mol·dm^{-3} nicotinic acid + 0.001 mol·dm^{-3} glycylglycine)

wavelength (λ_{max}) at 263, 213, 328, and 302 nm, respectively, while the UV–Vis spectrum shows two peaks at 293 and 460 nm for GP ligand. From the UV–Vis spectra in Figs. 7, 8, 9, 10, 11, 12, 13, 14, 15, 16, 17 and 18, we can conclude the following:

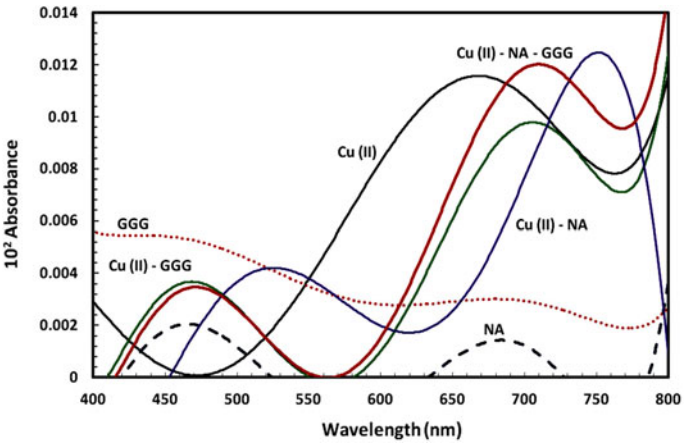

Fig. 9 Absorption spectra for (NA) nicotinic acid, (GGG) glycyl–glycyl–glycine, (Cu(II)–NA) binary system (0.001 mol·dm^{-3} Cu(II) + 0.001 mol·dm^{-3} nicotinic acid); (Cu(II)–GGG) binary system (0.001 mol·dm^{-3} Cu(II) + 0.001 mol·dm^{-3} glycyl–glycyl–glycine); (Cu(II)–NA–GGG) ternary system (0.001 mol·dm^{-3} Cu(II) + 0.001 mol·dm^{-3} nicotinic acid + 0.001 mol·dm^{-3} glycyl–glycyl–glycine)

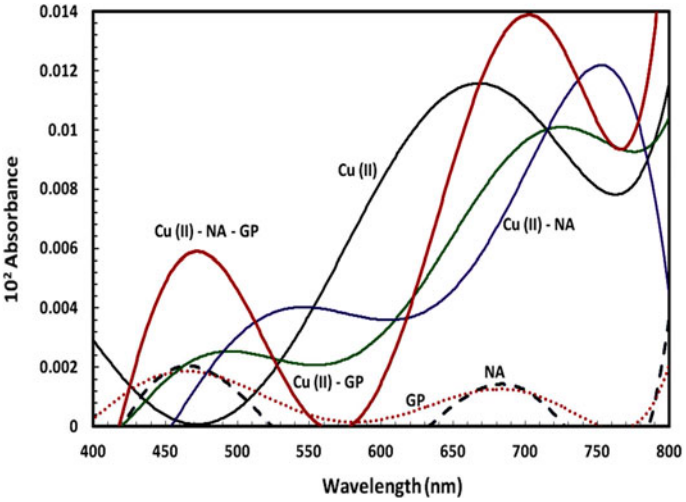

Fig. 10 Absorption spectra for (NA) nicotinic acid, (GP) glycyl-L-phenylalanine, (Cu(II)–NA) binary system (0.001 mol·dm^{-3} Cu(II) + 0.001 mol·dm^{-3} nicotinic acid); (Cu(II)–GP) binary system (0.001 mol·dm^{-3} Cu(II) + 0.001 mol·dm^{-3} glycyl-L-phenylalanine); (Cu(II)–NA–GP) ternary system (0.001 mol·dm^{-3} Cu(II) + 0.001 mol·dm^{-3} nicotinic acid + 0.001 mol·dm^{-3} glycyl-L-phenylalanine)

1. Each binary copper complex species involving the vitamin (NA) and G peptides (G; GG; GP and GGG), exhibited two maximum wavelengths (λ_{max}) at 525, 747 nm for CuNA; 473, 716 nm for CuG; 482, 713 nm for CuGG; 480, 705 nm for CuGGG; and 491, 714 nm for CuGP.
2. The mixed ligand nicotinic–copper complexes had two absorption maxima at 475, 710 nm for G; 480, 715 nm for GG; 480, 715 nm for GGG; and 471, 697 nm for GP.

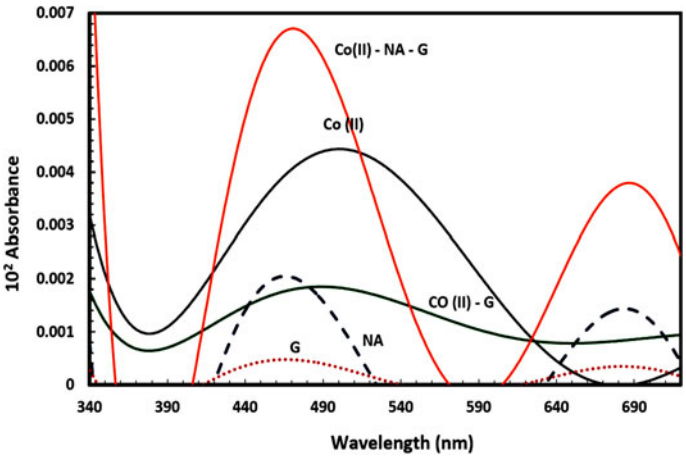

Fig. 11 Absorption spectra for (NA) nicotinic acid, (G) glycine; (Co(II)–G) binary system (0.001 mol·dm^{-3} Co(II) + 0.001 mol·dm^{-3} glycine); (Co(II)–NA–G) ternary system (0.001 mol·dm^{-3} Co(II) + 0.001 mol·dm^{-3} nicotinic acid + 0.001 mol·dm^{-3} glycine)

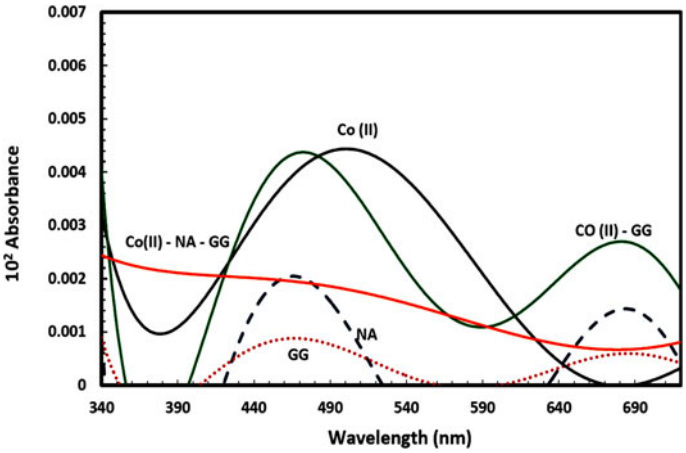

Fig. 12 Absorption spectra for (NA) nicotinic acid, (GG) glycylglycine; (Co(II)–GG) binary system (0.001 mol·dm^{-3} Co(II) + 0.001 mol·dm^{-3} glycylglycine); (Co(II)–NA–GG) ternary system (0.001 mol·dm^{-3} Co(II) + 0.001 mol·dm^{-3} nicotinic acid + 0.001 mol·dm^{-3} glycylglycine)

3. The binary cobalt complex species involving the vitamin (NA) and G peptides (G, GG, GP and GGG), exhibited one maximum at 513 nm for CoNA; 510 nm for CoGG; 504 nm for CoGGG; and two absorption maximum wavelengths at 511 nm for CoG.
4. The mixed ligand nicotinic–cobalt complex species showed one absorption maximum at 514 nm for the mixed complex species involving G; 484 nm for GG; and 507 nm for GP.
5. Each binary nickel complex species the vitamin (NA) and G peptides (G, GG, GP and GGG) demonstrated one maximum at 392 nm for NiNA; 394 nm for NiGG; 398 nm for NiGGG; 395 nm for NiGP; and two maxima at 386, 617 nm for NiG complexes.

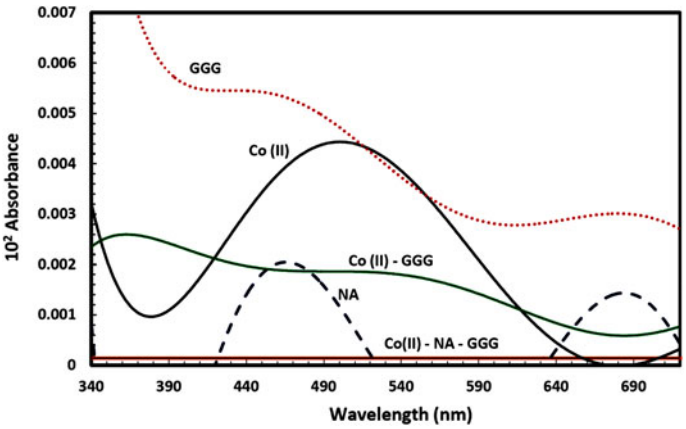

Fig. 13 Absorption spectra for (NA) nicotinic acid, (GGG) glycyl–glycyl–glycine; (Co(II)–GGG) binary system (0.001 mol·dm^{-3} Co(II) + 0.001 mol·dm^{-3} glycyl–glycyl–glycine); (Co(II)–NA–GGG) ternary system (0.001 mol·dm^{-3} Co(II) + 0.001 mol·dm^{-3} nicotinic acid + 0.001 mol·dm^{-3} glycyl–glycyl–glycine)

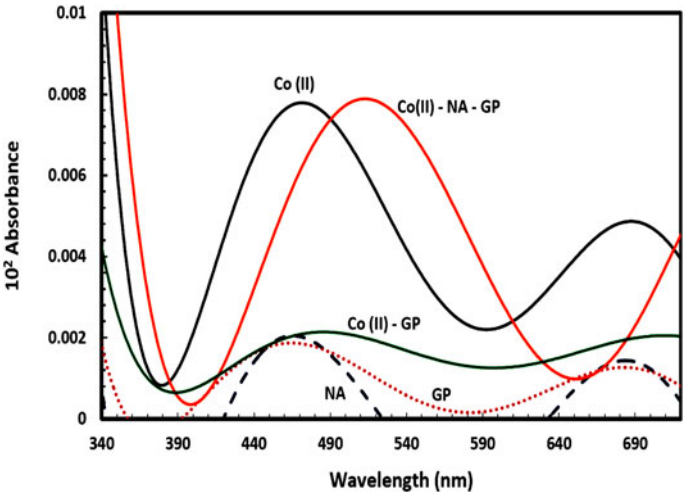

Fig. 14 Absorption spectra for (NA) nicotinic acid, (GP) glycyl-L-phenylalanine; (Co(II)–GP) binary system (0.001 mol·dm^{-3} Co(II) + 0.001 mol·dm^{-3} glycyl-L-phenylalanine); (Co(II)–NA–GP) ternary system (0.001 mol·dm^{-3} Co(II) + 0.001 mol·dm^{-3} nicotinic acid + 0.001 mol·dm^{-3} glycyl-L-phenylalanine)

6. The mixed ligand nicotinic–nickel complexes have one absorption maximum at 393 nm for G; 395 nm for GG; 390 nm for GGG; and 397 nm for GP.

3.5 Conductometric Titrations Analysis

The conductometric measurements of both binary and mixed ligand complexes were performed to examine the stoichiometries of the complex species formed in the solutions

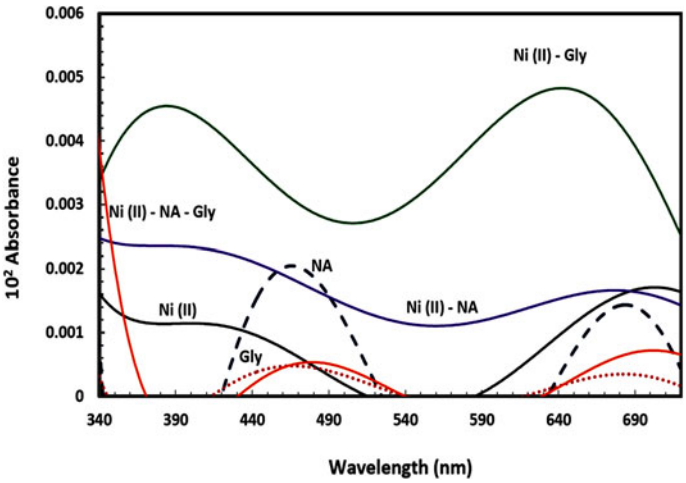

Fig. 15 Absorption spectra for (NA) nicotinic acid, (G) glycine, (Ni(II)–NA) binary system (0.001 mol·dm^{-3} Ni(II) + 0.001 mol·dm^{-3} nicotinic acid); (Ni(II)–G) binary system (0.001 mol·dm^{-3} Ni(II) + 0.001 mol·dm^{-3} glycine); (Ni(II)–NA–G) ternary system (0.001 mol·dm^{-3} Ni(II) + 0.001 mol·dm^{-3} nicotinic acid + 0.001 mol·dm^{-3} glycine)

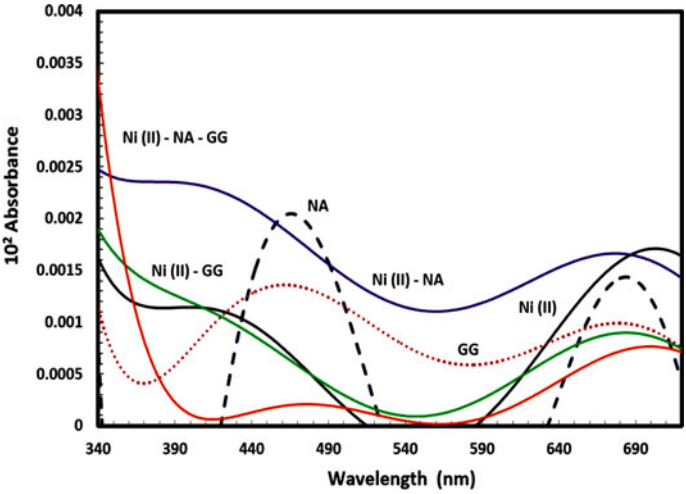

Fig. 16 Absorption spectra for (NA) nicotinic acid, (GG) glycylglycine, (Ni(II)–NA) binary system (0.001 mol·dm^{-3} Ni(II) + 0.001 mol·dm^{-3} nicotinic acid); (Ni(II)–GG) binary system (0.001 mol·dm^{-3} Ni(II) + 0.001 mol·dm^{-3} glycylglycine); (Ni(II)–NA–GG) ternary system (0.001 mol·dm^{-3} Ni(II) + 0.001 mol·dm^{-3} nicotinic acid + 0.001 mol·dm^{-3} glycylglycine)

from breaks denoting the formation of 1:1 binary metal ion complexes and 1:1:1 ternary complex. Conductometric titration curves for the binary and ternary complex species are shown in Figs. 19, 20, and in Figs. 24, 25, 26, 27 in Appendix 2. Some titration curves showed an initial decrease and an inflection at 0.5 and 1 mL of sodium hydroxide added for the binary systems, and only one inflection at 0.5 mL of base added for the ternary systems, followed by increasing conductance after the inflection point, due to the presence

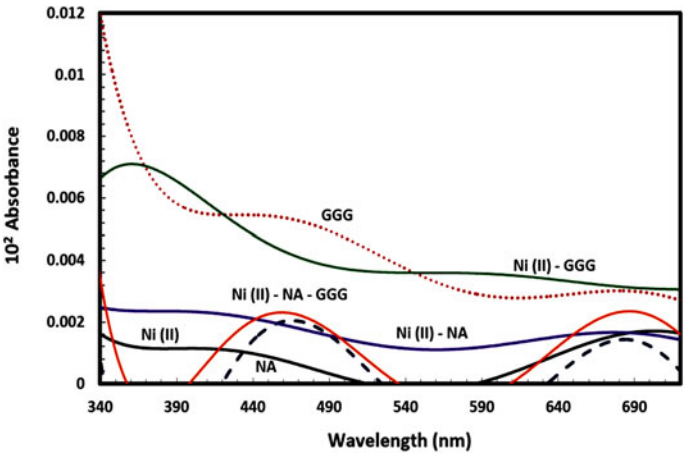

Fig. 17 Absorption spectra for (NA) nicotinic acid, (GGG) glycyl–glycyl–glycine, (Ni(II)–NA) binary system (0.001 mol·dm^{-3} Ni(II) + 0.001 mol·dm^{-3} nicotinic acid); (Ni(II)–GGG) binary system (0.001 mol·dm^{-3} Ni(II) + 0.001 mol·dm^{-3} glycyl–glycyl–glycine); (Ni(II)–NA–GGG) ternary system (0.001 mol·dm^{-3} Ni(II) + 0.001 mol·dm^{-3} nicotinic acid + 0.001 mol·dm^{-3} glycyl–glycyl–glycine)

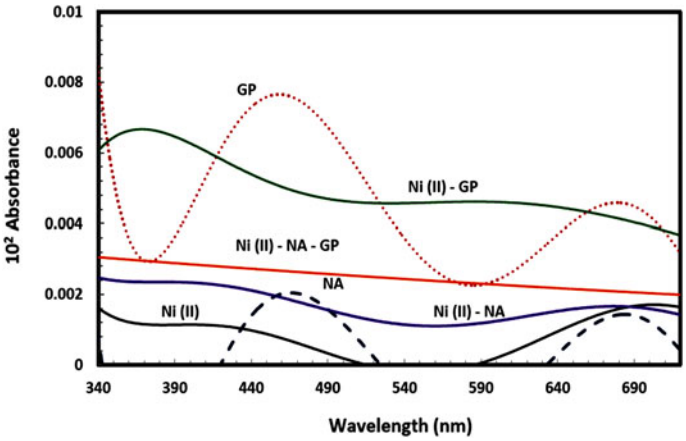

Fig. 18 Absorption spectra for (NA) nicotinic acid, (GP) glycyl-L-phenylalanine, (Ni(II)–NA) binary system (0.001 mol·dm^{-3} Ni(II) + 0.001 mol·dm^{-3} nicotinic acid); (Ni(II)–GP) binary system (0.001 mol·dm^{-3} Ni(II) + 0.001 mol·dm^{-3} glycyl-L-phenylalanine); (Ni(II)–NA–GP) ternary system (0.001 mol·dm^{-3} Ni(II) + 0.001 mol·dm^{-3} nicotinic acid + 0.001 mol·dm^{-3} glycyl-L-phenylalanine)

of excess base. The change of the molar conductance can be explained by the increase of the metal ion binary and ternary complexes, which is accompanied by a decrease in the diffusion coefficient and the lowering of the charge on the metal ion through bond formation with the ligand.

3.6 Cyclic Voltammetery

Typical cyclic voltammograms of the metal ions (Cu(II), and Co(II)) in the absence and presence of NA and G peptides (G, GG, GP, and GGG) are shown in Figs. 21 and 22,

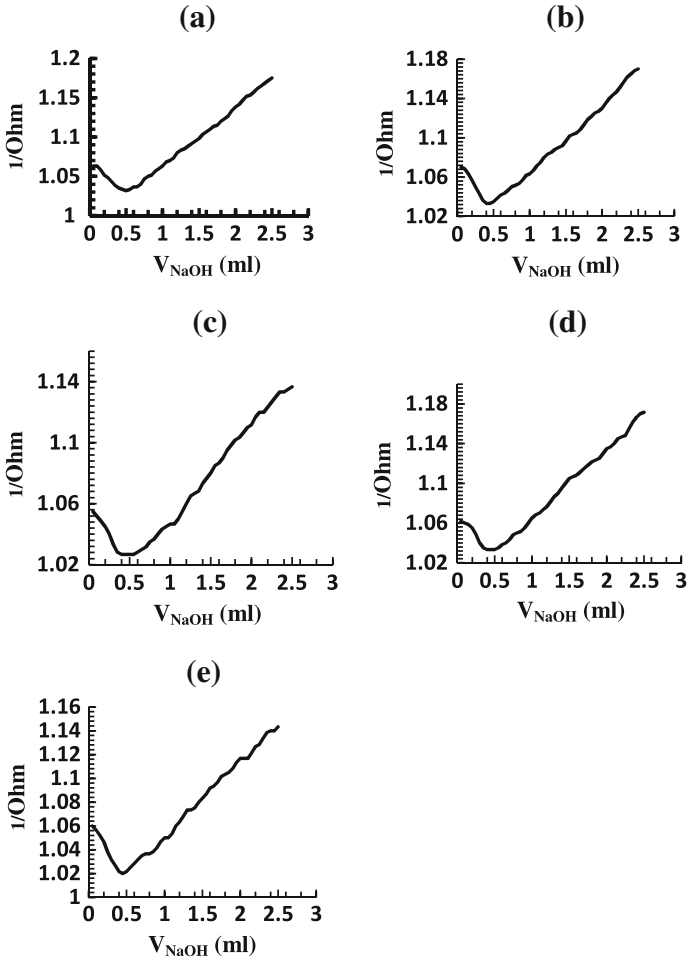

Fig. 19 Conductometric titration curves for **a** Cu(II)–NA, **b** Cu(II)–G, **c** Cu(II)–GG, **d** Cu(II)–GP and **e** Cu(II)–GGG binary systems at 0.16 mol·dm^{-3} $NaNO_3$ and 298.15 ± 0.1 K, [Cu(II)] = [NA] = [G] = [GG] = [GP] = [GGG] = 1 × 10^{-3} mol·dm^{-3}

under experimental conditions similar to those used in the potentiometric, conductometric and spectrophotometric measurements. The cyclic voltammograms demonstrate complex formation equilibria between copper, nickel, and cobalt metal ions and NA in the presence of G peptide units. The redox behavior of the copper and cobalt complexes was studied by cyclic voltammetric which is perhaps the most effective and versatile dynamic electrochemical technique available for mechanistic studies of redox systems. It enables the electrode potential to be rapidly scanned in search of redox couples. Once located, a couple can then be characterized from the potentials of peaks on the cyclic voltammograms and from changes caused by variation of the scan rate. In our cyclic voltammetric measurements, the electrode potential was varied linearly with time. The potential was measured between the reference electrode and the working electrode while the current is measured between the working electrode and the counter electrode. These data are shown in Figs. 21

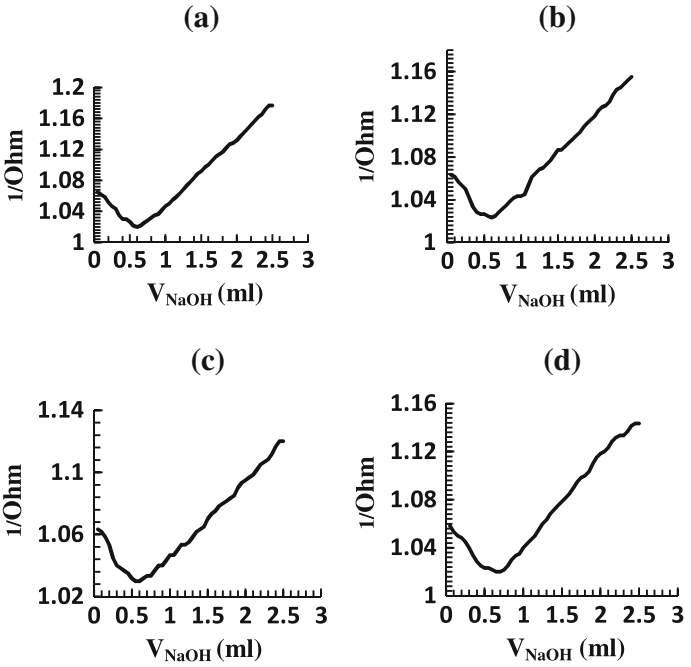

Fig. 20 Conductometric titration curves for **a** Cu(II)–NA–G, **b** Cu(II)–NA–GG, **c** Cu(II)–NA–GP, **d** Cu(II)–NA–GGG ternary systems at 0.16 mol·dm^{-3} $NaNO_3$ and 298.15 ± 0.1 K, [Cu(II)] = [NA] = [G] = [GG] = [GP] = [GGG] = 1 × 10^{-3} mol·dm^{-3}

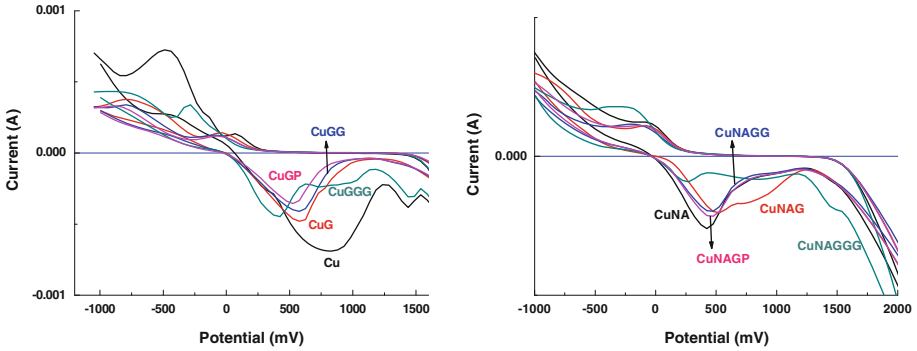

Fig. 21 Cyclic voltammetery diagrams for Cu(II) metal ion, Cu(II)–G, Cu(II)–GG, Cu(II)–GP, Cu(II)–GGG, Cu(II)–NA binary complexes, and Cu(II)–NA–G, Cu(II)–NA–GG, Cu(II)–NA–GG, Cu(II)–NA–GP, Cu(II)–NA–GGG ternary systems at I = 0.16 mol·dm^{-3} $NaNO_3$, T = 298.15 ± 0.1 K, [Cu(II)] = [NA] = [G] = [GG] = [GP] = [GGG] = 1 × 10^{-3} mol·dm^{-3}

and 22, where the oxidation peak usually has a similar shape to the reduction peak. Resulting from these measurements, information about the redox potential and electrochemical reaction rates of the complex species may be obtained. The cyclic voltammetric measurements showed only two quasi-reversible waves for each copper, nickel and cobalt

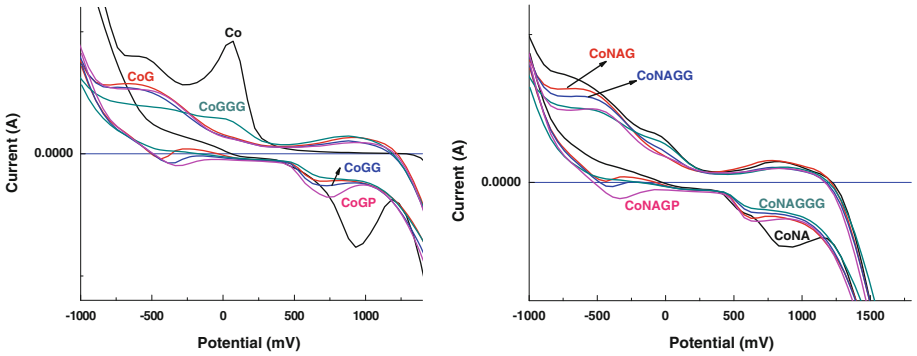

Fig. 22 Cyclic voltammetery diagrams for Co(II) metal ion, Co(II)–G, Co(II)–GG, Co(II)–GP, Co(II)–GGG, Co(II)–NA binary complexes, and Co(II)–NA–G, Co(II)–NA–GG, Co(II)–NA–GG, Co(II)–NA–GP, Co(II)–NA–GGG ternary systems at $I = 0.16$ mol·dm^{-3} $NaNO_3$, T = 298.15 ± 0.1 K, [Co(II)] = [NA] = [G] = [GG] = [GP] = [GGG] = 1×10^{-3} mol·dm^{-3}

complex species and they all showed redox couples with peak-to-peak separation values indicating a two step electron transfer process. By analysis of the cyclic voltammograms (Figs. 21, 22), the maximum current and potential in which charge transfer complexes were stable, and beyond that the charge transfer complexes get decomposed, were determined. Also, it is apparent that the most significant feature of the copper(II) complex is the Cu(II)/Cu(I) couple. The ratio of cathodic to anodic peak height was less than one. However, the peak current increases with the increase of the square root of the scan rates, establishing the diffusion control of the electrode process.

Acknowledgments This work was supported by King Abdulaziz City for Science and Technology (KACST) through the Project P–S-12-0017.

Appendix 1

See Fig. 23.

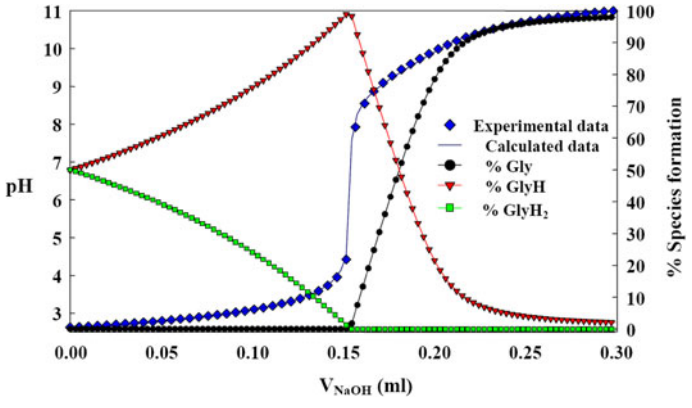

Fig. 23 Potentiometric titration and speciation diagram of glycine for protonation constants determination at $T = 298.15$ K and $I = 0.15$ mol·dm^{-3} $NaNO_3$

Appendix 2

See Figs. 24, 25, 26, 27.

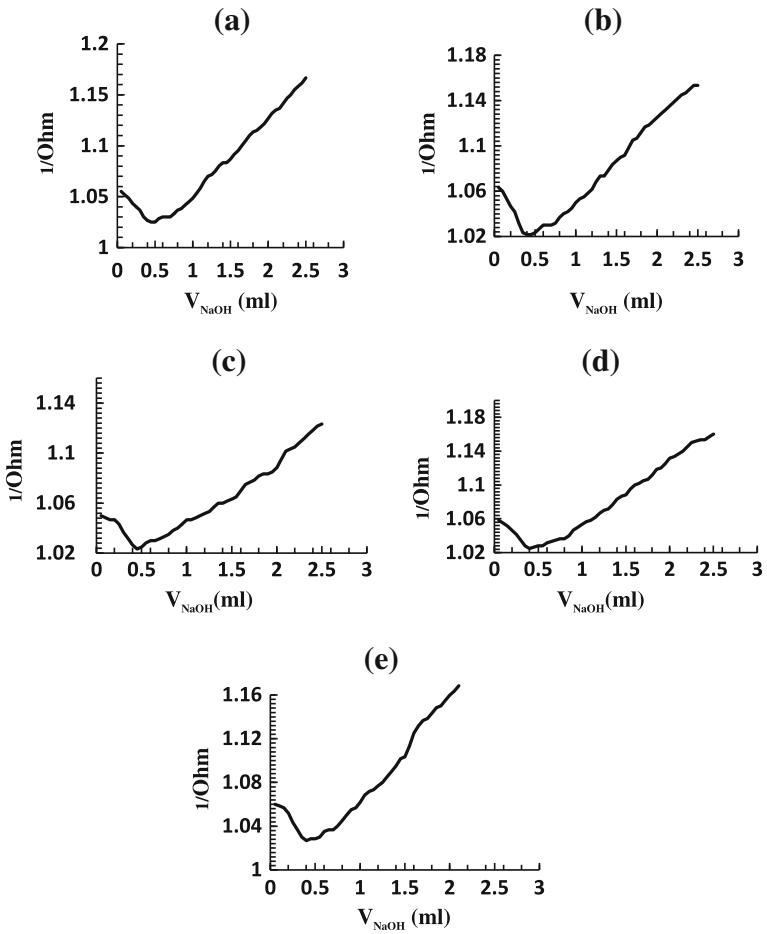

Fig. 24 Conductometric titration curves for **a** Co(II)–NA, **b** Co(II)–G, **c** Co(II)–GG, **d** Co(II)–GP and **e** Co(II)–GGG binary systems at $I = 0.16$ mol·dm^{-3} $NaNO_3$, $T = 298.15 \pm 0.1$ K, [Co(II)] = [NA] = [G] = [GG] = [GP] = [GGG] = 1×10^{-3} mol·dm^{-3}

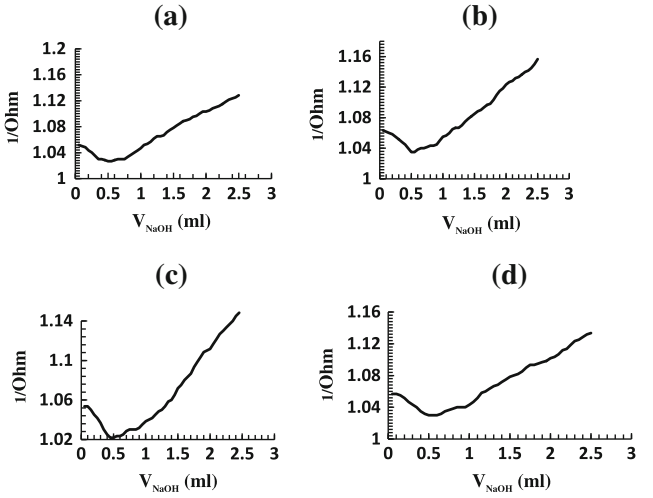

Fig. 25 Conductometric titration curves for **a** Co(II)–NA–G, **b** Co(II)–NA–GG, **c** Co(II)–NA–GG, **d** Co(II)–NA–GP and **e** Co(II)–NA–GGG ternary systems at $I = 0.16$ mol·dm^{-3} $NaNO_3$, $T = 298.15 \pm 0.1$ K, [Co(II)] = [NA] = [G] = [GG] = [GP] = [GGG] = 1×10^{-3} mol·dm^{-3}

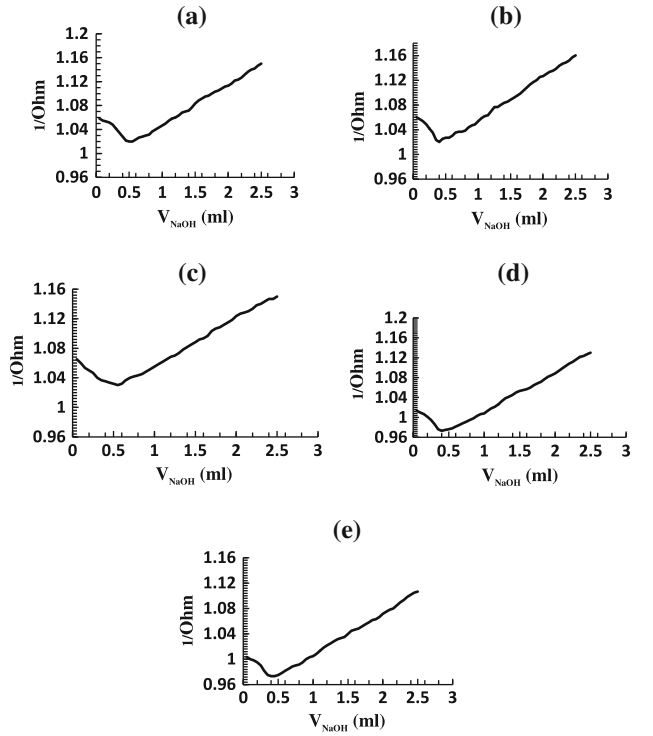

Fig. 26 Conductometric titration curves for **a** Ni(II)–NA, **b** Ni(II)–G, **c** Ni(II)–GG, **d** Ni(II)–GP and **e** Ni(II)–GGG binary systems at $I = 0.16$ mol·dm^{-3} $NaNO_3$, $T = 298.15 \pm 0.1$ K, [Ni(II)] = [NA] = [G] = [GG] = [GP] = [GGG] = 1×10^{-3} mol·dm^{-3}

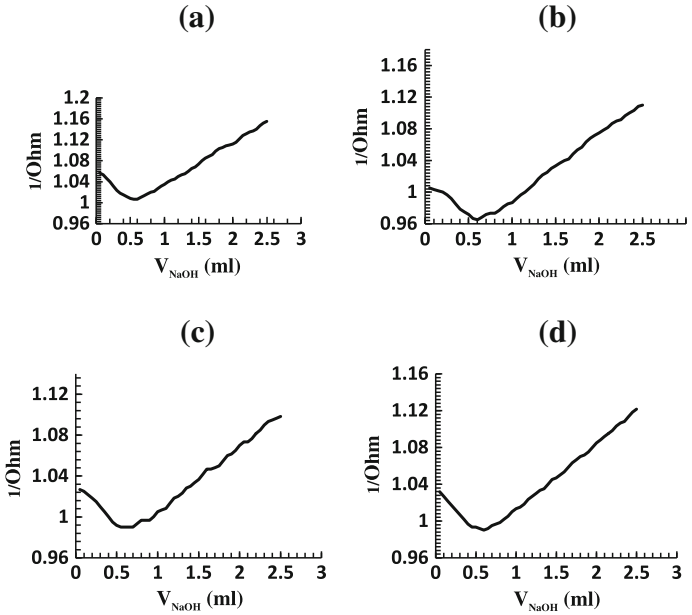

Fig. 27 Conductometric titration curves for **a** Ni(II)–NA–G, **b** Ni(II)–NA–GG, **c** Ni(II)–NA–GG, **d** Ni(II)–NA–GP and **e** Ni(II)–NA–GGG ternary systems at $I = 0.16$ mol·dm^{-3} $NaNO_3$, $T = 298.15 \pm 0.1$ K, [Ni(II)] = [NA] = [G] = [GG] = [GP] = [GGG] = 1×10^{-3} mol·dm^{-3}

References

1. Jacobson, E.L., Kim, H., Kim, M., Jacobson, M.K.: Niacin: vitamin and antidyslipidemic drug. Subcell. Biochem. **56**, 37–47 (2012)
2. Carlson, L.A.: Nicotinic acid: the broad-spectrum lipid drug. A 50th anniversary review. J. Intern. Med. **258**, 94–114 (2005)
3. Gonçalves, E.M., Bernardes, C.E.S., Diogo, H.P., Minas da Piedade, M.E.: Energetics and structure of nicotinic acid (niacin). J. Phys. Chem. B **114**, 5475–5485 (2010)
4. Offermanns, S.: The nicotinic acid receptor GPR109A (HM74A or PUMA-G) as a new therapeutic agent. Trends Pharmacol. Sci. **27**, 384–390 (2006)
5. Lorenzen, A., Stannek, C., Lang, H., Andrianov, V., Kalvinsh, I., Schwabe, U.: Characterization of a G-protein coupled receptor for nicotinic acid. Mol. Pharmacol. **59**, 349–357 (2001)
6. Villines, T.C., Kim, A.S., Gore, R.S., Taylor, A.J.: Niacin: the evidence, clinical use, and future directions. Curr. Atheroscler. Rep. **14**, 49–59 (2012)
7. Wise, A., Foord, S.M., Fraser, N.J., Barnes, A.A., Elshourbagy, N., Eilert, M., Ignar, D.M., Murdock, P.R., Steplewski, K., Green, A., Brown, A.J., Dowell, S.J., Szekeres, P.G., Hassall, D.G., Marshall, F.H., Wilson, S., Pike, N.B.: Molecular identification of high and low affinity receptors for nicotinic acid. J. Biol. Chem. **278**, 9869–9874 (2003)
8. Paolini, J.F., Mitchel, Y.B., Reyes, R., Kher, U., Lai, E., Watson, D.J., Norquist, J.M., Meehan, A.G., Bays, H.E., Davidson, M., Ballantyne, C.M.: Effects of laropiprant on nicotinic acid induced flushing in patients with dyslipidemia. Am. J. Cardiol. **101**, 625–630 (2008)
9. Sakai, T., Kamanna, V.S., Kashyap, M.L.: Niacin, but not gemfibrozil, selectively increases LP-AI, a cardioprotective subfraction of HDL, in patients with low HDL cholesterol. Arterioscler. Thromb. Vasc. Biol. **21**, 1783–1789 (2001)
10. Brown, B.G., Zhao, X.Q., Chait, A., Fisher, L.D., Cheung, M.C., Morse, J.S., Dowdy, A.A., Marino, E.K., Bolson, E.L., Alaupovic, P., Frohlich, J., Albers, J.J.: Simvastatin and niacin, antioxidant vitamins, or the combination for the prevention of coronary disease. New. Engl. J. Med. **345**, 1583–1592 (2001)

11. Angkawijaya, A.E., Fazary, A.E., Hernowo, E., Taha, M., Ju, Y.-H.: Iron(III), chromium(III), and copper(II) complexes of L-norvaline and ferulic acid. J. Chem. Eng. Data **56**, 532–540 (2011)
12. Fazary, A.E., Hernowo, E., Angkawijaya, A.E., Chou, T.-C., Lin, C.H., Taha, M., Ju, Y.-H.: Complex formation between ferric(III), chromium(III) and cupric(II) metal ions and (O, O) donor ligands with biological relevance in aqueous solution. J. Solution Chem. **40**, 1965–1986 (2011)
13. Hernowo, E., Angkawijaya, A.E., Fazary, A.E., Ismadji, S., Ju, Y.H.: Complex stability and molecular structure studies of divalent metal ion with L-norleucine and vitamin B3. J. Chem. Eng. Data **56**, 4549–4555 (2011)
14. Fazary, A.E., Taha, M., Ju, Y.H.: Iron complexation studies of gallic acid. J. Chem. Eng. Data **54**, 35–42 (2009)
15. Angkawijaya, A.E., Fazary, A.E., Ju, Y.H.: Cu(II), Co(II), and Ni(II)-antioxidative phenolates- glycine peptides systems: an insight into its equilibrium solution study. J. Chem. Eng. Data **57**, 3443–3451 (2012)
16. Angkawijaya, A.E., Fazary, A.E., Hernowo, E., Ismadji, S., Ju, Y.H.: Nickel and cobalt complexes of non-protein L-norvaline, and antioxidant ferulic acid: potentiometric and spectrophotometric studies. J. Solution Chem. **7**, 1156–1164 (2012)
17. Metrohm, AG.: Instructions for use for 6.6012.X40 Software TiNet 2.4 CH-9101 Herisau (Switzerland), pp. 1–148
18. Gans, P., Sabatini, A., Vacca, A.: Investigation of equilibria in solution, determination of equilibrium constants with the HYPERQUAD suite of programs. Talanta **43**, 1739–1753 (1996)
19. Alderighi, L., Gans, P., Ienco, A., Peters, D., Sabatini, A., Vacca, A.: Hyperquad simulation and speciation (HySS): a utility program for the investigation of equilibria involving soluble and partially soluble species. Coord. Chem. Rev. **184**, 311–318 (1999)
20. Frisch, M.J., Trucks, G.W., Schlegel, H.B., Scuseria, G.E., Robb, M.A., Cheeseman, J.R., Scalmani, G., Barone, V., Mennucci, B., Petersson, G.A., Nakatsuji, H., Caricato, M., Li, X., Hratchian, H.P., Izmaylov, A.F., Bloino, J., Zheng, G., Sonnenberg, J.L., Hada, M., Ehara, M., Toyota, K., Fukuda, R., Hasegawa, J., Ishida, M., Nakajima, T., Honda, Y., Kitao, O., Nakai, H., Vreven, T., Montgomery, J.A., Peralta, J.E., Ogliaro, F., Bearpark, M., Heyd, J.J., Brothers, E., Kudin, K.N., Staroverov, V.N., Kobayashi, R., Normand, J., Raghavachari, K., Rendell, A., Burant, J.C., Iyengar, S.S., Tomasi, J., Cossi, M., rega, N., Millam, J.M., Klene, M., Knox, J.E., Cross, J.B., Bakken, V., Adamo, C., Jaramillo, J., Gomperts, R., Stratmann, R. E., Yazyev, O., Austin, A.J., Cammi, R., Pomelli, C., Ochterski, J.W., Martin, E.L., Morokuma, K., Zakrzewski, V.G., Voth, G.A., Salvador, P., Dannenberg, J.J., Dapprich, S., Daniels, A.D., Farkas, O., Foresman, J.B., Ortiz, J.V., Cioslowski, J., Fox, D.J.: Gaussian 09 edn. Gaussian Inc., Wallingford (2009)
21. Becke, A.D.: Density-functional thermochemistry. III. The role of exact exchange. J. Chem. Phys. **98**, 5648–5652 (1993)
22. Lee, C., Yang, W., Parr, R.G.: Development of the Colle–Salvetti correlation-energy formula into a functional of the electron density. Phys. Rev. B **37**, 785–789 (1998)
23. Rassolov, V.A., Pople, J.A., Ratner, M.A., Windus, T.L.: 6-31G* basis set for atoms K through Zn. J. Chem. Phys. **109**, 1223–1229 (1998)
24. Ramos, J.M., Versiane, O.J.F., Soto, C.A.T.: Fourier transform infrared spectrum, vibrational analysis and structural determination of the trans-bis(glycine)nickel(II) complex by means of the RHF/6-311G and DFT:B3LYP/6-31G and 6-311G methods. Spectrochim. Acta Part A **68**, 1370–1378 (2007)
25. Ramos, J.M., Versiane, O., Felcman, J., Soto, C.A.T.: FT-IR vibrational spectrum and DFT:B3LYP/6-31G and B3LYP/6-311G structure and vibrational analysis of glycinate–guanidoacetate nickel(II) complex: [Ni(Gly)(Gaa)]. Spectrochim. Acta Part A **72**, 182–189 (2009)
26. Chachkov, D.V., Mikhailov, O.V.: DFT B3LYP calculation of the spatial structure of Co(II), Ni(II), and Cu(II) template complexes formed in ternary systems metal(II) ion–dithiooxamide–formaldehyde. Russ. J. Inorg. Chem. **54**, 1952–1956 (2009)
27. Kawakami, J., Miyamoto, R., Fukushi, A., Shimozaki, K., Ito, S.: Ab initio molecular orbital study of the complexing behavior of N-ethyl-1naphtalenecarboxamide as fluorescent chemosensors for alkali and alkaline earth metal ions. J. Photochem. Photobiol. A **146**, 163–168 (2002)
28. Gergely, A., Sovago, I., Nagypal, I., Kiraly, R.: Equilibrium relations of alpha-aminoacid mixed complexes of transition metal ions. Inorg. Chim. Acta **6**, 435–439 (1972)
29. Yamauchi, O., Hirano, Y., Nakao, Y., Nakahara, A.: Stability of fused rings in metal chelates. VI. Structures and stability constants of the copper(II) chelates of dipeptides containing glycine and/or β-alanine. Can. J. Chem. **47**, 3441–3445 (1969)
30. Yamauchi, O., Nakao, Y., Nakahara, A.: Stability of fused rings in metal chelates. X. Structures and stability constants of the copper(II) complexes of tripeptides composed of glycine and/or β-alanine. Bull. Chem. Soc. Japan **46**, 2119–2124 (1973)

31. Irving, H., Williams, R.J.P.: The stability of transition-metal complexes. J. Chem. Soc. **75**, 3192–3210 (1953)
32. Pagenkopf, G.K., Margerum, D.W.: Proton-transfer reaction with copper(II)–triglycine (CuH-2L-). J. Am. Chem. Soc. **90**, 501–502 (1968)
33. Basolo, F., Chen, Y.T., Murmann, R.K.: Sterric effects and the stability of complex compounds. IV. The chelating tendencies of C-substituted ethylenediamines with copper(II) and nickel(II) ions. J. Am. Chem. Soc. **76**, 956–959 (1954)
34. Lenarcik, B., Kierzkowska, A.: The influence of alkyl chain length and steric effect on stability constants and extractability of Zn(II) complexes with 1-alkyl-4(5)-methylimidazoles. Sep. Sci. Technol. **39**, 3485–3508 (2004)
35. Sigel, H., Prijs, B., Martin, R.B.: Stability of binary and ternary β-alanine containing dipeptide copper(II) complexes. Inorg. Chim. Acta **56**, 45–49 (1981)
36. Turkel, N., Sahin, C.: Stability of binary and ternary copper(II) complexes with 1,10-phenanthroline, 2,2′-bipyridyl and some α-amino acids in aqueous medium. Chem. Pharm. Bull. **57**, 694–699 (2009)
37. Khade, B.C., Deore, P.M., Arbad, B.R.: Mixed-ligand complex formation of copper(II) with some aminoacids and drug dapsone. Int. J. ChemTech Res. **2**, 1036–1041 (2010)
38. Sharifi, S., Nori-shargha, D., Bahadory, A.: Complexes of thallium(I) and cadmium(II) with dipeptides of L-phenylalanylglycine and glycyl-L-phenylalanine. J. Braz. Chem. Soc. **18**, 1011–1016 (2007)
39. Casale, A., Robertis, A.D., Stefano, C.D., Gianguzza, A., Patane, G., Rigano, C., Sannartano, S.: Thermodynamic parameters for the formation of glycine complexes with magnesium(II), calcium(II), lead(II), manganese(II), cobalt(II), nickel(II), zinc(II) and cadmium(II) at differenr temperatures and ionic strengths, with particular reference to natural fluid conditions. Thermochim. Acta **255**, 109–141 (1995)
40. Erdemgil, F.Z., Sanli, S., Sanli, N., Ozkan, G., Barbosa, J., Guiteras, J., Beltran, J.L.: Determination of p*K*a values of some hydroxylated benzoic acids in methanol–water binary mixtures by LC methodology and potentiometry. Talanta **72**, 489–496 (2007)
41. Wu, C.D., Lu, C.Z., Zhuang, H.H., Huang, J.S.: Structure and magnetic property of a new 3D nicotinic acid bridged nickel polymer. Z. Anorg. Allg. Chem. **629**, 693–696 (2003)
42. Ahuja, I.S., Singh, R., Rai, C.P.: Complexes of copper(II) with nicotinic acid and some related ligands. Transit. Met. Chem. **2**, 257–260 (1977)
43. Cooper, J.A., Anderson, B.F., Buckley, P.D., Blackwell, L.F.: Structure and biological activity of nitrogen and oxygen coordinated nicotinic acid complexes of chromium. Inorg. Chim. Acta **91**, 1–9 (1984)
44. Abu-Youssef, M.A.M.: Two new 3D network structures: $[Cd_3(nic)_4(N_3)_2(H_2O)]_n$ and $[Zn(nic)(N_3)]n$ (nic = nicotinate anion). Polyhedron **24**, 1829–1836 (2005)
45. Pearson, R.J.: Hard and soft acids and bases. J. Am. Chem. Soc. **85**, 3533–3539 (1963)